

20 min at a flow rate of 3  $\mu\text{L}/\text{min}$ . Mass spectra were recorded with a Finnigan LTQ system (Thermo Fisher Scientific, Waltham, MA) using sequential scan events: MS ( $m/z$  450–2000) followed by data-dependent MS/MS on the IT-MS for the most intense ions in positive ion mode. For protein identification, all obtained product ions were subjected to a computer database search analysis with the TurboSEQUEST search engine (Thermo Fisher Scientific) using the Swiss-Prot database and search parameters: a static modification of carboxyamidomethylation (57 Da) at Cys and trypsin for digestion.

**Extraction and Proteinase Digestion of the 45–70 kDa Proteins Separated by SDS-PAGE.** The gel-separated proteins were extracted as previously reported (28). The proteins were extracted with 20 mM Tris-HCl containing 1% SDS by being shaken vigorously overnight after the gel had been broken down into small bits. The extract was filtered with Ultrafree-MC (0.22  $\mu\text{m}$ ; Millipore, Bedford, MA), and the proteins were precipitated via addition of cold acetone. The resulting precipitate was digested with endoproteinase Glu-C (3.75  $\mu\text{g}$ ) in 30  $\mu\text{L}$  of 0.1 M ammonium acetate (pH 8.0) at 37  $^{\circ}\text{C}$  for 4 days, followed by incubation with additional trypsin (1  $\mu\text{g}$ ) at 37  $^{\circ}\text{C}$  overnight.

**LC-MS<sup>n</sup>.** Proteolytic peptides were separated by reversed-phase columns, Magic C30 and C18 (50 mm  $\times$  0.1 mm, 3  $\mu\text{m}$ ; Michrom BioResources), and a graphitized carbon column (GCC), Hypercarb 5  $\mu$  (150 mm  $\times$  0.2 mm; Thermo Fisher Scientific), with a Paradigm MS4 HPLC system consisting of pump A with 0.1% formic acid and 2% acetonitrile and pump B with 0.1% formic acid and 90% acetonitrile. For analysis of glycopeptides, separation was performed with a linear gradient from 5 to 50% pump B over 100 min followed by a 50 to 95% B gradient over 10 min and 95% B over 10 min at a flow rate of 0.5  $\mu\text{L}/\text{min}$ , and mass spectra were recorded with a Finnigan LTQ-FT system (Thermo Fisher Scientific) using sequential scan events: MS ( $m/z$  1000–2000 or 700–2000) with the IT-MS followed by MS with the IT-MS-FT ICR-MS in selected ion monitoring (SIM) mode and data-dependent MS<sup>n</sup> with the IT-MS for the most intense ions. The LC-MS<sup>n</sup> runs were performed with a C30 column and scan range of  $m/z$  1000–2000 (condition A), twice, with a C30 column and scan range of  $m/z$  700–2000 (condition B), once, and with a C18 column and scan range of  $m/z$  1000–2000 (condition C), once. For analysis of GPI-linked peptides, separation was performed with a linear gradient from 5 to 60% pump B over 100 min at a flow rate of 2  $\mu\text{L}/\text{min}$  for a GCC, and mass spectra were recorded with a Finnigan LTQ system using sequential scans: a single mass scan ( $m/z$  700–2000) with the IT-MS followed by data-dependent MS<sup>n</sup> scans with the IT-MS for the most intense ions, twice. LC-MS<sup>n</sup> was performed using a capillary voltage of 1.8 kV and a capillary temperature of 200  $^{\circ}\text{C}$ .

## RESULTS

**Preparation of Lipid-Free IgLON Glycopeptides.** Figure 2 illustrates the experimental procedure for the glycosylation analysis of IgLON family proteins. Lipid-free GPI-linked proteins in a rat brain tissue sample were enriched via phase partitioning with Triton X-114 and PIPLC digestion. The enriched proteins were separated by SDS-PAGE and stained

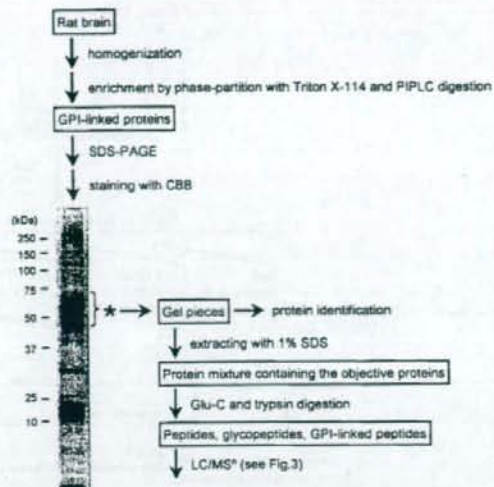


FIGURE 2: Experimental procedure for site-specific glycosylation analysis of IgLON family proteins and SDS-PAGE (12.5%) of lipid-free GPI-linked proteins which were enriched from rat brain. The asterisk indicates the gel band containing IgLON family proteins.

with Coomassie Brilliant Blue. The presence of LAMP, OBCAM, neurotrimin, and Kilon in the gel band at 45–70 kDa was confirmed by in-gel trypsin digestion followed by LC-MS/MS. The IgLON proteins were extracted with other comigrated proteins from 45–70 kDa bands in other lanes by being shaken in 1% SDS. After SDS had been removed, the mixture of proteins was digested with endoproteinase Glu-C and trypsin. Most of the resulting glycopeptides contained only a single N-glycosylation site, with the exception of LGTTN<sup>270</sup>ASLPLNPPSTAQYGITG<sup>287</sup> in Kilon, which included a predicted GPI attachment site at Gly287 in addition to a potential N-glycosylation site at Asn270 (Figure 1). The glycopeptides from IgLON family proteins was separated by using three different columns: a reversed-phase column, a C30 and a C18 column for hydrophobic glycopeptides, and a GCC for hydrophilic glycopeptides, including GPI-linked peptides.

**Glycosylation Analysis of LAMP.** LC-MS analysis was performed via MS on the IT-MS and data-dependent MS in SIM mode on the FT ICR-MS, and data-dependent MS/MS and MS/MS/MS were performed on the IT-MS in the positive ion mode (Figure 3). After MS data acquisition, the MS/MS spectrum (scan  $n$ ) of a glycopeptide was selected manually from all MS data on the basis of the existence of carbohydrate distinctive fragments, such as Hex<sub>1</sub>HexNAc<sub>1</sub><sup>+</sup> ( $m/z$  366) and Hex<sub>1</sub>HexNAc<sub>1</sub>NeuAc<sup>+</sup> ( $m/z$  657). Then a set of the glycopeptide's MS data consisting of the mass spectrum (scan  $n - 2$ ), the mass spectrum in SIM on the FT ICR-MS (scan  $n - 1$ ), the MS/MS spectrum (scan  $n$ ), and the MS/MS/MS spectrum (scan  $n + 1$ ) was selected from all the MS data (step 1). The carbohydrate structure was deduced from the fragment ions appearing in the MS/MS spectrum (scan  $n$ ), and the peptide portion was estimated from the peptide-related ions (step 2). The sequences of some peptides were confirmed by the b- and y-ions that arose from Y<sub>1</sub> ([peptide + HexNAc + H]<sup>+</sup>) in MS/MS/MS (scan  $n +$

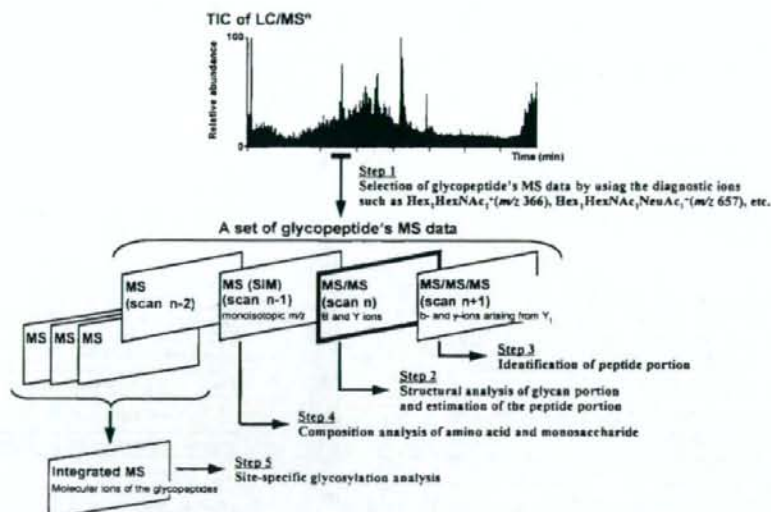


FIGURE 3: Methods used for LC-MS<sup>n</sup> and data analysis.

1) (step 3). The accurate molecular mass that was calculated from the monoisotopic  $m/z$  value and the charge state acquired by FT ICR-MS in SIM mode (scan  $n - 1$ ) was used to corroborate the assignment of the peptide and glycan moieties (step 4). The mass spectra acquired at the elution position, where the glycopeptides that yielded identical  $Y_1$  ions in the MS/MS and/or MS/MS/MS spectra, were integrated, and the site-specific glycosylation was elucidated on the basis of the distribution of molecular ions in the integrated mass spectra (step 5). As a representative separation pattern, a total ion chromatogram (TIC) obtained by LC-MS<sup>n</sup> with a C30 column (scan range of  $m/z$  1000–2000) is shown in Figure 4A. The MS/MS spectra containing the diagnostic ions at  $m/z$  366 and 657 were picked out from all the MS data, and the peptides eluted at positions 1–25 were determined to be the glycopeptides on the basis of the carbohydrate-related ions. The 19% of spectra acquired at elution time, including positions 1–25, could be traced back to the glycopeptides of IgLON family proteins.

As for LAMP, it has seven potential N-glycosylation sites at Asn12, -38, -108, -120, -251, -259, and -272, and Asn287 is the predicted site of GPI linkage. On the basis of the presence of the peptide-related ions ([peptide + HexNAc + H]<sup>+</sup>,  $Y_1$  or  $Y_{1\alpha/\beta}$ ; or [peptide + dHex-HexNAc + H]<sup>+</sup>,  $Y_{1\alpha}$ ), glycopeptides that were eluted at the positions 1, 11, 14, 12, 4, and 24 were estimated to be the glycopeptides containing Asn12, -38, -108, -251, -259, and -272, respectively. The MS/MS spectra of the glycopeptide containing Asn120 (GSN<sup>120</sup>VTLVCMANGRPE) were not acquired in any of the runs. However, glycosylation at Asn120 was confirmed by the detection of the peptide substituted with Asp (GSD<sup>120</sup>VTLVCMANGRPEPVITWR) after PNGase F digestion (data not shown). Panels A1–F1 of Figure 5 show the representative MS/MS and MS/MS/MS spectra acquired at positions 11, 1, 14, 12, 4, and 24, respectively. The integrated mass spectra of the glycopeptides containing Asn38, -12, -108, -251, -259, and -272 are shown in panels A2–F2 of Figure 5, respectively. The feature of the

glycosylation at each glycosylation site was elucidated on the basis of these MS spectra.

(i) *Asn38 (Asn43 in OBCAM and Asn38 in neurotrimin)*. Panel A1 of Figure 5 shows one of the MS/MS spectra acquired at position 11. The peptide portion, VAWL(GlcNAc)<sub>N</sub><sup>38</sup>R, was confirmed on the basis of the b- and y-ions that arose from  $Y_1$  ( $m/z$  961.5) in the MS/MS/MS spectrum (panel A1' of Figure 5). A series of doubly charged Y ions with an  $m/z$  spacing pattern, 81  $m/z$  units (Hex), suggests the linkage of Man-7 to this peptide. The attachment of Man-7 to VAWLN<sup>38</sup>R, whose theoretical monoisotopic  $m/z$  value ( $[M + 2H]^{2+}$ ) is 1149.983, was ascertained by the observed monoisotopic  $m/z$  value (1149.986) acquired in SIM mode on the FT ICR-MS (panel A1' of Figure 5). Panel A2 of Figure 5 shows the integrated mass spectrum which was obtained from the mass spectra of glycopeptides that yielded  $Y_1$  ( $m/z$  961.5) via MS/MS. Four noticeable ion peaks (peaks a-1–a-4) appearing with the differences of 81  $m/z$  units are assigned to VAWLN<sup>38</sup>R glycosylated with Man-6-9 (Table 1A). The MS/MS spectra of DKNSKVAVLN<sup>38</sup>R and CVVEDKNSKVAVLN<sup>38</sup>R, which were picked out from positions 9 and 15, also revealed that Man-5, -7, and -8 were attached to Asn38.

(ii) *Asn12*. Panel B1 of Figure 5 shows the representative MS/MS spectrum of glycopeptide, GTDN<sup>12</sup>ITVR, which was selected from position 1. From the  $Y_{1\alpha}$  ion ( $m/z$  1224.5) together with monoisotopic  $m/z$  value of the molecular ion ( $m/z$  1173.132) and a series of doubly charged Y ions with an  $m/z$  spacing pattern, 146 (NeuAc), 101 (HexNAc), and 81  $m/z$  units (Hex), the carbohydrate portion was estimated to be dHex<sub>1</sub>Hex<sub>2</sub>HexNAc<sub>2</sub>NeuAc<sub>4</sub>. Furthermore, a complex-type oligosaccharide, to which one branch of disialic acid was attached, was deduced from the presence of  $B_{4\alpha}/Y_{5\alpha}$  ( $m/z$  495.3),  $B_{2\alpha}$  ( $m/z$  582.7),  $B_{3\alpha}$  ( $m/z$  744.9),  $B_{4\alpha}/Y_{5\alpha}$  and  $B_{4\alpha}/Y_{1\alpha}$  ( $m/z$  948.2), and  $B_{4\alpha}$  ( $m/z$  1239.5) (inset of panel B1 of Figure 5). The integrated mass spectrum at position 1 suggests that the majority of the glycans at Asn12 are hybrid- and complex-type oligosaccharides containing disialic acids

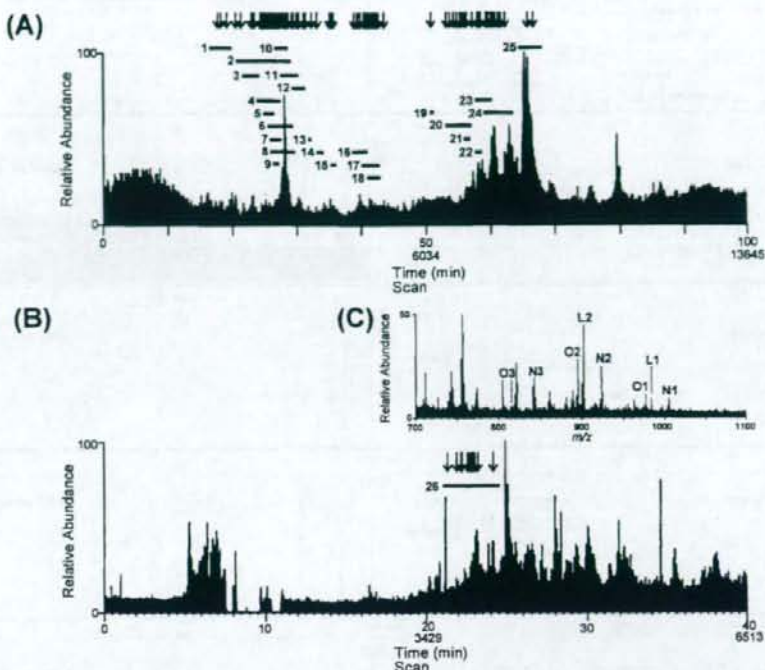


FIGURE 4: Total ion chromatograms obtained by C30-LC-MS<sup>a</sup> (A) and GCC-LC-MS<sup>a</sup> (B). Lines 1–25 and 26 are the elution positions of glycopeptides and GPI-linked peptides, respectively. The down arrow denotes the extracted position of the MS/MS spectra. (C) Integrated mass spectrum obtained from elution position 26. L1 and L2 are molecular ions of GPI-linked peptides from LAMP, N1–N3 those from neurotmin, and O1–O3 those from OBCAM.

(panel B2 of Figure 5 and Table 1B). In addition, the partial glycosylation at Asn12 was indicated by the detection of nonglycosylated GTDN<sup>12</sup>ITVR.

(iii) *Asn108*. The MS/MS spectrum of glycosylated ISN<sup>108</sup>ISSDVTYNE ( $Y_{1\alpha/1\beta}$ ,  $m/z$  1480.6) acquired at position 14 is shown in panel C1 of Figure 5. The attachment of a Lewis *a/x* [ $Le^{a/x}$ , Gal-(Fuc)-GlcNAc-] or H antigen (Fuc-Gal-GlcNAc-) motif to the bisected complex-type oligosaccharide was deduced from the monosaccharide composition (dHex<sub>2</sub>Hex<sub>4</sub>HexNAc<sub>5</sub>) and the  $Le^{a/x}$  and H antigen-related ion ( $m/z$  512.1) and  $Y_{1\beta\alpha/1\beta}^{2+}$  ( $m/z$  1024.3) (panel C1 of Figure 5, peak c-1 in panel C2 of Figure 5). The alternative LC-MS<sup>a</sup> run with the C30 column (scan range of  $m/z$  1000–2000) suggested that ISN<sup>108</sup>ISSD is also occupied by sialyl  $Le^{a/x}$  (s $Le^{a/x}$ )-modified or core-fucosylated hybrid-type oligosaccharides based on the presence of NeuAc-Hex-(dHex-)-HexNAc<sup>+</sup> ( $m/z$  803.1), Hex-(dHex-)-HexNAc<sup>+</sup> ( $m/z$  512.3), NeuAc-Hex<sup>+</sup> ( $m/z$  454.2), and [peptide + dHex + HexNAc + H]<sup>+</sup> ( $m/z$  1084.3) (data not shown, Table 1C).

(iv) *Asn251*. The representative MS/MS spectrum of the glycopeptide containing GQSSLTVTN<sup>251</sup>VTE ( $Y_{1\alpha/1\beta}$ ,  $m/z$  1438.6; elution position 12) is shown in panel D1 of Figure 5. From the monoisotopic mass and the  $Le^{a/x}$ -related ions ( $m/z$  350.3 and 512.2), the carbohydrate structure was estimated to be a complex-type oligosaccharide to which the  $Le^{a/x}$  motif was attached (dHex<sub>2</sub>Hex<sub>4</sub>HexNAc<sub>5</sub>; inset of panel D1 of Figure 5). Other glycans at Asn251 were characterized as complex-type oligosaccharides containing s $Le^{a/x}$  or Lewis b/y [ $Le^{b/y}$ , Fuc-Gal-(Fuc)-GlcNAc-] based on the molecular

ions in the integrated mass spectrum (peaks d-1–6 in panel D2 of Figure 5), the s $Le^{a/x}$ -related ions ( $m/z$  803, 657, and 512), and the  $Le^{b/y}$ -related ions ( $m/z$  658.2, 512.1, and 350.2) acquired by the alternative run with the C30 column (scan range of  $m/z$  700–2000) (Table 1D).

(v) *Asn259*. Panel E1 of Figure 5 shows the product ion spectra of HYGNT<sup>259</sup>YTCVAANK linked by dHex<sub>2</sub>Hex<sub>2</sub>HexNAc<sub>5</sub>, which was deduced from the  $Y_{1\alpha/1\beta}$  ion ( $m/z$  1600.6) and the monoisotopic mass acquired at position 4. The BA-2, which is a core-fucosylated and agalactobiantennary oligosaccharide with bisecting GlcNAc, and known as a brain-specific carbohydrate, was suggested by the product ions at  $m/z$  1085.3 (bisecting GlcNAc) and 1746.6 (core-fucosylation) (inset of panel E1 of Figure 5). The majority of other glycans at Asn259 were characterized as  $Le^{a/x}$ -modified complex and hybrid types. Man-5 was suggested to be a minor glycan (panel E2 of Figure 5 and Table 1E).

(vi) *Asn272*. Panel F1 of Figure 5 shows the MS/MS and MS/MS/MS spectra of glycopeptide LGVTN<sup>272</sup>ASLVLFRR ( $Y_{1\alpha/1\beta}$ ,  $m/z$  1492.8), which were acquired at position 24. The monosaccharide composition (dHex<sub>2</sub>Hex<sub>4</sub>HexNAc<sub>5</sub>) and the presence of  $Y_{3\alpha/3\beta}^{2+}$  ( $m/z$  1103.8) and  $Le^{a/x}$ -related ion suggested the attachment of a  $Le^{a/x}$  or H antigen motif to the bisected and core-fucosylated complex-type oligosaccharide (inset of panel F1 of Figure 5). The MS/MS spectra of the LGVTN<sup>272</sup>ASLVLFRRPGSVR glycopeptides ( $Y_{1\alpha/1\beta}^{2+}$ ,  $m/z$  1069) were also picked out at position 24 (data not shown). The  $m/z$  values of molecular ions appearing in the

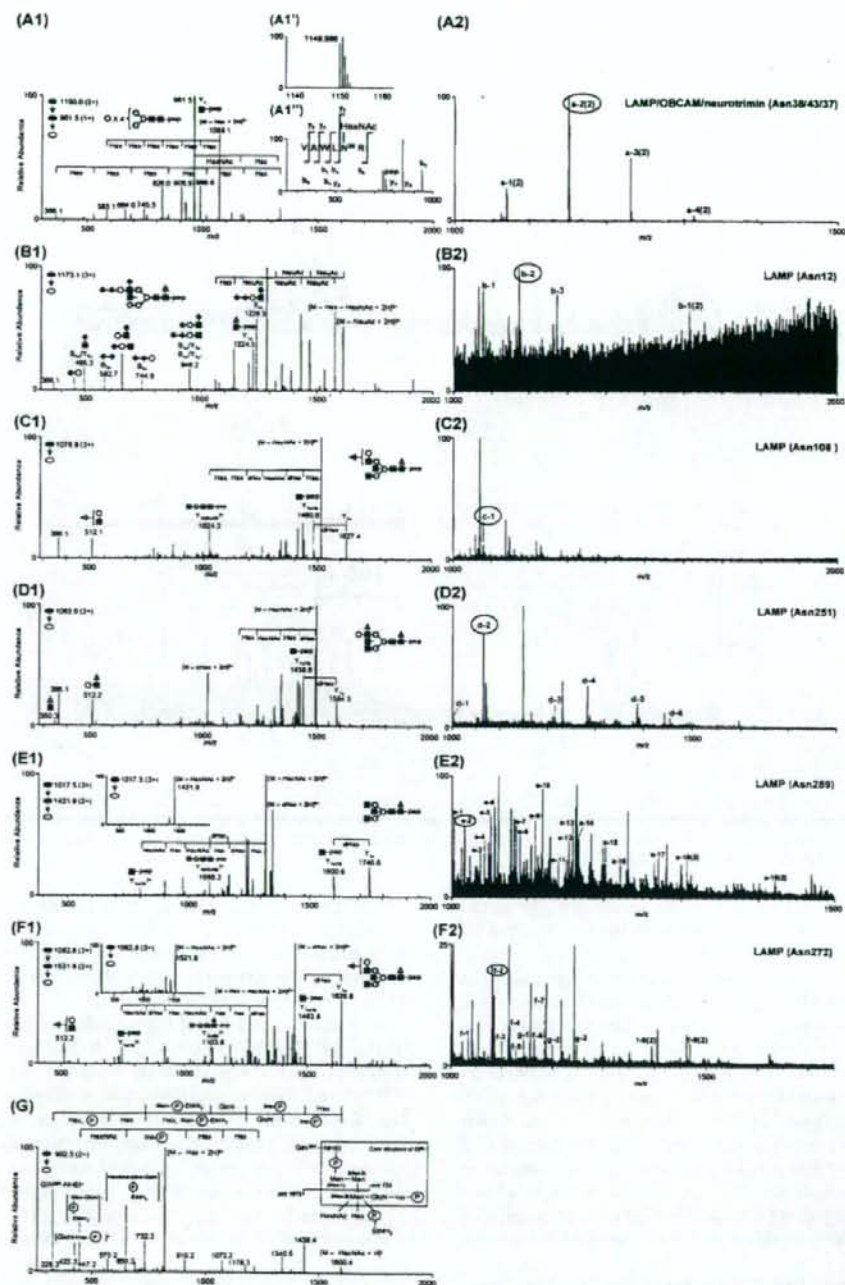


FIGURE 5: MS spectra of LAMP glycopeptides. (A1) MS/MS spectrum of glycopeptide VAWLN<sup>38</sup>R; elution position, 11; precursor ion,  $[M + 2H]^{2+}$  ( $m/z$  1150.0). (A1') Mass spectrum on the FT ICR-MS in SIM mode. (A1'') MS/MS spectrum acquired from Y<sub>1</sub> ( $m/z$  961.5). (A2) Integrated mass spectrum obtained from position 11. (B1) MS/MS spectrum of glycopeptide GTDN<sup>121</sup>TVR; elution position, 1; precursor ion,  $[M + 3H]^{3+}$  ( $m/z$  1173.1). (B2) Integrated mass spectrum at position 1. (C1) MS/MS spectrum of glycopeptide ISN<sup>108</sup>ISSDVTVNE; elution position, 14; precursor ion,  $[M + 3H]^{3+}$  ( $m/z$  1078.8). (C2) Integrated mass spectrum at position 14. (D1) MS/MS spectrum of glycopeptide GQSSLTVTN<sup>251</sup>VTE; elution position, 12; precursor ion,  $[M + 3H]^{3+}$  ( $m/z$  1065.0). (D2) Integrated mass spectrum at position 12. (E1) MS/MS and MS/MS/MS spectra of glycopeptide HYGN<sup>259</sup>YTCVAANK; elution position, 4; precursor ion,  $[M + 3H]^{3+}$  ( $m/z$  1017.5). (E2) Integrated mass spectrum at position 4. (F1) MS/MS and MS/MS/MS spectra of glycopeptide LGVTN<sup>277</sup>ASLVLFRR; elution position, 24; precursor ion,  $[M + 3H]^{3+}$  ( $m/z$  1082.8). (F2) Integrated mass spectrum at position 24. (G) MS/MS spectrum of GPI-linked GIN<sup>267</sup>; elution position, 26; precursor ion,  $[M + 2H]^{2+}$  ( $m/z$  902.5). Symbols are as in Figure 9.

Table 1: Summary of Glycosylation Analysis of IgLON Family Proteins

protein	peptides	glycopeptides							N-glycan					
		sequence <sup>a,b</sup>	elution position	Figure	peak no. <sup>c</sup>	scan in Figure 4A <sup>d</sup>	observed peptide-related ion <sup>e</sup>	observed m/z in SIM mode <sup>b</sup>	theoretical m/z <sup>b</sup>	deduced monosaccharide composition				deduced structure <sup>f</sup> (diagnostic ion)
										dHex	Hex	HexNAc	NA	
LAMP	B	GTDN <sup>121</sup> TVR (874.451)	1	5, B2	b-1	2095 (A, B)	1225.4	1076.101 (3)	1076.101	1	5	4	2	H, CoreF(1225.4)
					b-1 (2)	2146	1225.6	1613.652 (2)	1613.648	1	5	4	2	H, CoreF(1225.6)
					b-2	2166 (A, B, C)	1224.5	1173.132 (3)	1173.133	1	5	4	3	H, CoreF(1224.5), diSia(582.7) [Figure 5, B1]
					– (A)	1224.5	1759.195 (2)	1759.196	1	5	4	3	CoreF(1224.5), diSia(583.0)	
					b-3	2235 (A)	1224.5	1270.166 (3)	1270.165	1	5	4	4	C, CoreF(1224.5), diSia(583.0)
					– (A)	1225.6	1367.199 (3)	1367.196	1	5	4	5	C, CoreF(1225.6), diSia(583.4)	
	A	VAWLN <sup>98</sup> R (757.424)	11	5, A2	– (B)	961.5	987.930 (2)	987.930	0	5	2	0	Man-5	
					a-1 (2)	3523 (A, B, C)	961.5	1068.956 (2)	1068.957	0	6	2	0	Man-6
					a-2 (2)	3364 (A, B, C)	961.5	1149.986(2)	1149.983	0	7	2	0	Man-7 [Figure 5, A1]
					a-3 (2)	3221 (A, B, C)	961.5	1231.010 (2)	1231.010	0	8	2	0	Man-8
					a-4 (2)	3413 (A, B, C)	961.5	1312.039 (2)	1312.036	0	9	2	0	Man-9
					–	3074	1534.8	1011.774 (3)	1011.773	0	8	2	0	Man-8
C	DKNSKVAWLN <sup>98</sup> R (1329.715) CVVEDKNSKVAWLN <sup>98</sup> R (1816.925)	9	–	–	4298	675.5(3)	1012.128 (3)	1012.123	0	5	2	0	Man-5	
				–	4245	1011.2(2)	1120.160 (3)	1120.159	0	7	2	0	Man-7	
				–	4208	1011.3(2)	1174.175 (3)	1174.176	0	8	2	0	Man-8	
				– (A)	938.4	1296.508 (2)	1296.507	1	5	3	1	H, CoreF(1084.3) or sL <sup>MH</sup> (454.2, 512.3, 657.2, 803.1)		
				– (A)	938.5	1377.533 (2)	1377.534	1	6	3	1	H, CoreF(1084.2)		
				– (A)	3963	1480.6	1078.456 (3)	1078.454	2	4	5	0	C, CoreF(1627.4), bisectGN(1024.3) [Figure 5, C1] glycosylated <sup>g</sup>	
D	GSN <sup>120</sup> VTLVCMANGRPEPVITWR (1603.745) GQSSLTVTN <sup>231</sup> VTE (1234.604)	12	5, D2	– (A)	1438.6	1340.576 (2)	1340.576	1	3	4	0	CoreF(1584.6), bisectGN(1003.6)		
				– (A)	1438.5	961.746 (3)	961.746	1	3	5	0	C, CoreF(1584.5), bisectGN(1004.1), BA-2		
				– (A, B)	1438.5	1442.115 (2)	1442.116	1	3	5	0	C, CoreF(1584.5), bisectGN(1077.2), BA-2		
				d-1	3630	1438.5	1002.088 (3)	1002.088	1	5	4	0	H, CoreF(1584.5) or L <sup>MH</sup> (350.1, 512.1)	
				d-2	3646 (A, B, C)	1438.6	1064.451 (3)	1064.450	2	4	5	0	C, CoreF(1584.5), L <sup>MH</sup> (350.3, 512.2) [Figure 5, D1]	
				– (C)	1439.6	1596.174 (2)	1596.171	2	4	5	0	C, CoreF(1585.6), 512(512.2)		
				– (B)	1438.5	1167.154 (3)	1167.154	3	5	5	0	C, CoreF(1584.5), bisectGN(1004.1), L <sup>MH</sup> (350.2, 512.1, 658.2)		
				d-3	3742 (C)	1438.6	1215.502 (3)	1215.499	2	5	5	1	C, CoreF(1584.4), 512(512.3)	
				d-4	3788 (C)	1438.6	1283.192 (3)	1283.193	2	5	6	1	C, CoreF(1584.5) (sL <sup>MH</sup> (512.2, 657.2, 803.2))	
				d-5	3668	1438.6	1385.898 (3)	1385.896	3	6	6	1	C, CoreF(1584.5) (sL <sup>MH</sup> (512.2, 657.3, 803.1))	
				d-6	3618 (A)	1438.5	1453.594 (3)	1453.589	3	6	7	1	C, CoreF(1584.6), 512(512.2)	

Table 1: Continued

protein	peptides		glycopeptides					N-glycan					
	sequence <sup>a,b</sup>	elution position	Figure	peak no. <sup>c</sup>	scan in Figure 4A <sup>d</sup>	observed peptide-related ion <sup>e</sup>	observed m/z in SIM mode <sup>b</sup>	theoretical m/z <sup>b</sup>	deduced monosaccharide composition				deduced structure <sup>f</sup> (diagnostic ion)
									dHex	Hex	HexNAc	NA	
E	HYGN <sup>299</sup> YTCVAANK (1396.619)	4	5, E2		— (B)	801.8(2)	872.021 (3)	872.021	0	5	2	0	Man-5
				e-18 (2)	2884	1600.6	1307.532 (2)	1307.528	0	5	2	0	Man-5
				e-19 (2)	2949 (A)	1601.4	1421.587 (2)	1421.584	1	3	4	0	CoreF(1746.7), bisectGN(1085.6)
				e-1	2891 (A, C)	1600.6	1002.079 (3)	1002.076	1	4	4	0	H, CoreF(1746.6), bisectGN(1085.3)
				e-2	2931 (A, B, C)	1600.6	1015.752 (3)	1015.752	1	3	5	0	C, CoreF(1746.6), bisectGN(1085.3), BA-2 (Figure 5, E1)
				e-3	2859 (A)	1600.5	1037.089 (3)	1037.086	2	5	3	0	H, CoreF(1746.6), 512(512.1)
				e-4	2840	1600.6	1042.419 (3)	1042.418	1	6	3	0	H, 512(512.1)
				e-5	2878 (A)	1601.6	1050.764 (3)	1050.762	2	4	4	0	CoreF(1746.6), L <sup>MA</sup> (350.2, 512.2), bisectGN(1085.5)
				e-6	2853 (A, B, C)	1600.5	1056.095 (3)	1056.094	1	5	4	0	H, CoreF(1747.7), bisectGN(1085.6)
				e-7	2994	1600.7	1085.433 (3)	1085.432	1	5	3	1	H, CoreF(1747.6) or 512(512.2)
				e-8	2821	1600.5	1091.107 (3)	1091.104	2	6	3	0	H, CoreF(1746.6), 512(512.2)
					— (A, C)	1601.6	1104.779 (3)	1104.780	2	5	4	0	H, CoreF(1747.8), bisectGN(1158.7), L <sup>MA</sup> (349.9, 512.3)
				e-9	2847	1600.6	1110.111 (3)	1110.111	1	6	4	0	H, CoreF(1746.6) or L <sup>MA</sup> (350.1, 512.3)
				e-10	2898 (A, C)	1601.7	1118.457 (3)	1118.455	2	4	5	0	C, CoreF(1746.7), bisectGN(1085.7), L <sup>MA</sup> (350.2, 512.1)
				e-11	2989	1600.7	1139.452 (3)	1139.450	1	6	3	1	H, CoreF(1746.7)
				e-12	2808 (A)	1600.6	1153.467 (3)	1153.466	3	5	4	0	C, CoreF(1746.6), L <sup>MB</sup> (658.2) or 512/512(512.1/ 512.3)
				e-13	2872	1600.4	1158.798 (3)	1158.797	2	6	4	0	H, CoreF(1747.7), L <sup>MA</sup> (350.1, 512.1)
e-14	3036	1601.7	1166.800 (3)	1166.801	1	4	5	1	C, CoreF(1747.4) or 512(512.1), bisectGN(1085.3)				
e-15	2983	1600.6	1201.813 (3)	1201.811	2	5	4	1	C, CoreF(1747.6), sL <sup>MA</sup> (350.1, 512.2, 657.3, 803.2)				
e-16	2815	1600.6	1221.160 (3)	1221.159	3	5	5	0	C, CoreF(1747.6), bisectGN(1085.3), 512(512.2)				
e-17	3013	1600.7	1269.507 (3)	1269.505	2	5	5	1	C, CoreF(1746.7), bisectGN(1085.5), 512(512.1)				

Table 1: Continued

protein	peptides sequence <sup>a,b</sup>	elution position	Figure	glycopeptides				N-glycan							
				peak no. <sup>c</sup>	scan in Figure 4A <sup>d</sup>	observed peptide- related ion <sup>e</sup>	observed <i>m/z</i> in SIM mode <sup>b</sup>	theoretical <i>m/z</i> <sup>b</sup>	deduced monosaccharide composition				deduced structure/ (diagnostic ion)		
									dfHex	Hex	HexNAc	NA			
F	LGVTN <sup>772</sup> ASLVLFR (1288.750)	24	5, F2	– (B)		1492.8	931.109 (3)	1396.160	0	3	5	0	C, bisectGN(1030.9)		
				f-8 (2)	7644 (A, B)	1492.8	1396.161 (2)	1396.160	0	3	5	0	C, bisectGN(1031.0)		
					– (B)			1492.8	979.795 (3)	979.795	1	3	5	0	C, CoreF(1638.9), bisectGN(1031.2), BA-2
				f-9 (2)	7577 (A, B, C)	1492.7	1469.189 (2)	1469.189	1	3	5	0	C, CoreF(1638.8), bisectGN(1031.2), BA-2		
					– (A, B, C)			1492.9	1014.806 (3)	1014.806	2	4	4	0	C, CoreF(1640.0), 512(512.3)
				f-1	7558 (A, B, C)	1493.7	1033.813 (3)	1033.813	1	4	5	0	C, bisectGN(1031.1), CoreF(1639.8) or L <sup>NA</sup> (350.2, 512.2)		
					– (A)			1493.8	1550.215 (2)	1550.215	1	4	5	0	C, bisectGN(1031.6), CoreF(1640.0) or 512(512.2)
					– (A)			1492.9	1047.489 (3)	1047.488	1	3	6	0	C, CoreF(1638.8), bisectGN(1031.7)
					– (A, C)			1492.9	1063.151 (3)	1063.151	1	4	4	1	C, CoreF(1638.9)
					– (A)			1492.9	1082.157 (3)	1082.159	0	4	5	1	C, bisectGN(1031.0)
				f-2	7468 (A, B, C)	1492.8	1082.499 (3)	1082.499	2	4	5	0	C, CoreF, bisectGN(1103.8) [Figure 5, F1]		
					– (A)			1492.8	1623.243 (2)	1623.244	2	4	5	0	C, CoreF(1638.9), bisectGN(1031.0), 512(513.2)
				f-3	7382 (A)	1492.8	1101.510 (3)	1101.506	1	4	6	0	C, bisectGN(1031.2), CoreF(1639.0) or L <sup>NA</sup> (350.3, 512.2)		
				f-4	7753 (A, B, C)	1492.7	1117.168 (3)	1117.169	1	5	4	1	C, CoreF(1638.8) or sL <sup>NA</sup> (454.2, 512.3, 657.2, 803.1)		
					– (A)			1493.9	1675.247 (2)	1675.250	1	5	4	1	H, CoreF(1638.9)
					– (A)			1493.8	1117.508 (3)	1117.509	3	5	4	0	C, CoreF(1639.4), L <sup>NA</sup> (512.2, 658.5)
				f-5	7889 (A, C)	1492.8	1130.846 (3)	1130.845	1	4	5	1	C, CoreF(1638.7), bisectGN(1031.0, 1104.3)		
					– (A)			1492.9	1136.517 (3)	1136.516	2	5	5	0	C, CoreF(1639.8), 512(512.2)
					– (A)			1494.0	1150.192 (3)	1150.192	2	4	6	0	C, CoreF(1639.1), L <sup>NA</sup> (350.1, 512.2)
					– (A)			1493.1	1165.516 (3)	1165.515	0	5	4	2	C
				f-6	7815 (A, B, C)	1492.6	1165.856 (3)	1165.855	2	5	4	1	C, CoreF(1638.7), sL <sup>NA</sup> (453.8, 512.1, 657.1, 803.2)		
					– (A)			1493.3	1748.280 (2)	1748.279	2	5	4	1	C, CoreF(1639.9), 512(512.3)
				f-7	7765	1493.9	1184.864 (3)	1184.862	1	5	5	1	C, bisectGN(1032.0), CoreF(1639.3) or 512(512.2)		
					– (A, C)			1492.7	1185.202 (3)	1185.202	3	5	5	0	C, CoreF(1639.1), L <sup>NA</sup> (512.2, 658.4)
					– (A)			1492.7	1204.209 (3)	1204.209	2	5	6	0	C, CoreF(1638.9), L <sup>NA</sup> (350.2, 512.2)
					– (A, C)			1493.2	1214.201 (3)	1214.201	1	5	4	2	C, CoreF(1639.8)

Table 1: Continued

protein	peptides sequence <sup>a,b</sup>	elution position	Figure	glycopeptides			N-glycan				deduced structure <sup>f</sup> (diagnostic ion)		
				peak no. <sup>c</sup>	scan in Figure 4A <sup>d</sup>	observed peptide- related ion <sup>e</sup>	observed m/z in SIM mode <sup>b</sup>	theoretical m/z <sup>b</sup>	deduced monosaccharide composition				
									dHex	Hex		HexNAc	NA
LGVTN <sup>272</sup> ASLVLFPPGVS (1785.026)		24	5, F2	— (A)		1493.8	1233.548 (3)	1233.548	2	5	5	1	C, CoreF(1639.1), sL <sup>hA</sup> (454.0, 512.6, 657.1, 803.0)
				— (A)		1493.8	1287.567 (3)	1287.566	2	6	5	1	C, CoreF(1639.4), 512(512.3)
				— (C)		1492.7	1336.251 (3)	1336.252	3	6	5	1	C, CoreF, 512(512.4)
				— (C)		1492.7	1384.602 (3)	1384.598	2	6	5	2	C, CoreF(1638.8) (sL <sup>hA</sup> ) (454.9, 512.3, 657.1, 803.3)
				— (C)		995.3(2)	1096.537 (3)	1096.534	0	3	5	0	C, bisectGN(1279.5)
				g-1	7508 (C)	995.4(2)	1145.223 (3)	1145.220	1	3	5	0	C, CoreF(1068.7), bisectGN(1352.3), BA-2
				g-2	7462 (C)	995.8(2)	1199.243 (3)	1199.238	1	4	5	0	C, CoreF(1069.2) or 512(512.2)
				g-3	7449 (C)	995.9(2)	1247.927 (3)	1247.924	2	4	5	0	C, CoreF(1068.4), bisectGN(1279.4), 512(512.2)
				— (C)		995.8(2)	1282.596 (3)	1282.594	1	5	4	1	C, 512(512.2)
				— (C)		995.4(2)	1331.283 (3)	1331.280	2	5	4	1	C, CoreF(1068.4), 512(512.3)
OBCAM G AMDN <sup>17</sup> VTVR (904.444)		2	6, A2	h-1	2408 (A)	1254.5	1018.407 (3)	1018.405	1	5	3	2	H, CoreF(1254.5), (diSia(583.0))
				— (A, C)		1254.7	1086.098 (3)	1086.099	1	5	4	2	CoreF(1254.7)
				— (A)		1254.5	1628.644 (2)	1628.644	1	5	4	2	C, CoreF(1254.5)
				— (A, B)		1254.7	1115.437 (3)	1115.437	1	5	3	3	H, CoreF(1254.7), diSia(583.0)
				— (A)		1254.5	1672.651 (2)	1672.652	1	5	3	3	H, CoreF(1254.5), diSia(583.3)
				— (A)		1254.6	1169.454 (3)	1169.455	1	6	3	3	H, CoreF(1254.6), diSia(583.0)
				h-2	2473 (A, B, C)	1254.5	1183.131 (3)	1183.130	1	5	4	3	H, CoreF(1254.5) or 512(512.2), diSia(582.6)
				h-3	2719 (C)	1254.5	1280.163 (3)	1280.162	1	5	4	4	C, CoreF(1254.5), diSia(582.9) [Figure 6, A1]
				— (C)		1108.6	1377.198 (3)	1377.194	1	5	4	5	Man-5
				— (B)		961.5	987.930 (2)	987.930	0	5	2	0	Man-6
A VAWLN <sup>43</sup> R (757.424)		11	5, A2	a-1 (2)	3523 (A, B, C)	961.5	1068.956 (2)	1068.957	0	6	2	0	Man-7 [Figure 5, A1]
				a-2 (2)	3364 (A, B, C)	961.5	1149.986(2)	1149.983	0	7	2	0	Man-8
				a-3 (2)	3221 (A, B, C)	961.5	1231.010 (2)	1231.010	0	8	2	0	Man-9
				a-4 (2)	3413 (A, B, C)	961.5	1312.039 (2)	1312.036	0	9	2	0	glycosylated <sup>g</sup>
	VHLIVQVPPQIMN <sup>113</sup> ISSD (1889.008)	—	—	—	—	—	—	—	—	—	—	glycosylated <sup>g</sup>	
	VHLIVQVPPQIMN <sup>113</sup> ISSDITVNE (2445.294)	—	—	—	—	—	—	—	—	—	—	glycosylated <sup>g</sup>	
H ISTLTFN <sup>233</sup> VSE (1256.629)		25	6, B2	— (A)		1460.6	1351.589 (2)	1351.589	1	3	4	0	CoreF(1606.3), bisectGN(1087.8)
				— (B)		1460.5	969.088 (3)	969.088	1	3	5	0	C, CoreF(1606.5), bisectGN(1088.6), BA-2
				— (A, C)		1461.5	1453.128 (2)	1453.128	1	3	5	0	C, CoreF(1606.5), bisectGN(1088.4), BA-2



Table 1: Continued

protein	peptides		glycopeptides					N-glycan					
	sequence <sup>a,b</sup>	elution position	Figure	peak no. <sup>c</sup>	scan in Figure 4A <sup>d</sup>	observed peptide-related ion <sup>e</sup>	observed m/z in SIM mode <sup>b</sup>	theoretical m/z <sup>b</sup>	deduced monosaccharide composition				deduced structure <sup>f</sup> (diagnostic ion)
									dHex	Hex	HexNAc	NA	
I	YGN <sup>266</sup> YTCVATNK (1289.571)	7	6, C2	- (A, B, C)		1461.7	1071.792 (3)	1071.792	2	4	5	0	C, (CoreF(1606.5), L <sup>NA</sup> (350.1, 512.2)) or (L <sup>NA</sup> (658.4))
				- (A, C)		1460.5	1607.183 (2)	1607.184	2	4	5	0	C, 512(512.3)
				- (C)		1460.5	1120.138 (3)	1120.137	1	4	5	1	C, CoreF(1606.5)
				- (A, C)		1460.5	1155.148 (3)	1155.148	2	5	4	1	C, CoreF(1606.6) (sL <sup>NA</sup> (349.2, 512.2, 804.1))
				- (A, B)		1460.5	1174.494 (3)	1174.495	3	5	5	0	C, CoreF(1606.5), L <sup>NA</sup> (350.7, 512.3, 658.2)
				- (A, C)		1461.4	1187.831 (3)	1187.831	1	4	6	1	C, CoreF(1606.6) or sL <sup>NA</sup> (350.1, 512.5, 657.1, 803.1)
				- (C)		1460.5	1222.842 (3)	1222.841	2	5	5	1	C, CoreF(1606.5), sL <sup>NA</sup> (454.0, 512.2, 803.2)
				i-1	8712 (A, B, C)	1460.5	1290.538 (3)	1290.534	2	5	6	1	C, CoreF(1606.6) (sL <sup>NA</sup> (454.2, 512.2, 657.1, 803.3)) [Figure 6, B1]
				i-2	8541 (A, C)	1460.5	1393.239 (3)	1393.238	3	6	6	1	C, CoreF(1606.5), 512(512.2)
				- (A)		1493.6	1254.003 (2)	1254.004	0	5	2	0	Man-5
				- (A)		1493.6	1368.060 (2)	1368.060	1	3	4	0	CoreF(1639.6), bisectGN(1031.5)
				- (B)		1493.6	980.068 (3)	980.069	1	3	5	0	C, CoreF(1639.6), bisectGN(1032.2), BA-2
				j-4 (2)	3156 (A, B, C)	1493.6	1469.602 (2)	1469.599	1	3	5	0	C, CoreF(1639.6), bisectGN(1105.0), BA-2
				- (C)		1493.6	1015.082 (3)	1015.079	2	4	4	0	CoreF(1639.5), L <sup>NA</sup> (350.2, 512.1), bisectGN(1105.1)
				j-1	3048 (A)	1494.6	1082.774 (3)	1082.772	2	4	5	0	C, CoreF(1640.5), L <sup>NA</sup> (350.4, 512.2), bisectGN(1105.9) [Figure 6, C1]
j-2	3030	1493.6	1117.783 (3)	1117.783	3	5	4	0	H, CoreF(1639.5), L <sup>NA</sup> (350.3, 512.1, 658.1)				
j-3	3024	1494.6	1185.478 (3)	1185.476	3	5	5	0	C, CoreF(1639.6), L <sup>NA</sup> (349.0, 512.1), bisectGN(1032.7)				
DYGN <sup>266</sup> YTCVATNK (1404.598)	13	-	- (A)		1608.6	1311.517 (2)	1311.518	0	5	2	0	Man-5	
			3885 (A)		1609.7	1018.412 (3)	1018.411	1	3	5	0	C, CoreF(1754.5), bisectGN(1089.6), BA-2	
			- (A)		1608.6	1527.113 (2)	1527.113	1	3	5	0	C, CoreF(1754.6), bisectGN(1089.1), BA-2	
			- (A)		1608.6	1121.115 (3)	1121.115	2	4	5	0	C, CoreF(1754.7), L <sup>NA</sup> (350.3, 512.3)	
			- (A)		1608.7	1156.125 (3)	1156.125	3	5	4	0	H, CoreF(1754.8), 512(512.2)	
KDYGN <sup>266</sup> YTCVATNK (1532.693)	6	-	- (C)		1736.7	1489.625 (2)	1489.621	1	3	4	0	CoreF(1882.8), bisectGN(1225.1)	
			3510 (C)		1737.8	1061.109 (3)	1061.109	1	3	5	0	C, CoreF(1884.9), bisectGN(1226.7), BA-2	
			3133		1737.7	1150.141 (3)	1150.137	2	5	4	0	H, CoreF(1883.8), L <sup>NA</sup> (350.4, 512.2)	

Table 1: Continued

protein	peptides		glycopeptides					N-glycan				deduced structure/ (diagnostic ion)		
	sequence <sup>a,b</sup>	elution position	Figure	peak no. <sup>c</sup>	scan in Figure 4A <sup>d</sup>	observed peptide-related ion <sup>e</sup>	observed m/z in SIM mode <sup>b</sup>	theoretical m/z <sup>b</sup>	deduced monosaccharide composition					
									dHex	Hex	HexNAc		NA	
neurotrophin	LGNTN <sup>178</sup> ASITLYGPGVAID (1774.910)	-	-	-	(C)	1736.5	1163.814 (3)	1163.813	2	4	5	0	C, CoreF(1882.7), bisectGN(1153.7), L <sup>NA</sup> (350.3, 512.2)	
					3054	1737.6	1198.826 (3)	1198.823	3	5	4	0	C, CoreF(1884.7), L <sup>NA</sup> (350.1, 512.2)	
					3458	1737.1	1212.160 (3)	1212.159	1	4	5	1	C, CoreF(1883.9), bisectGN(1226.3)	
					3295	1737.0	1247.170 (3)	1247.169	2	5	4	1	CoreF(1882.8), sL <sup>NA</sup> (453.8, 512.2, 657.2, 803.2)	
					(A)	1978.7	1093.161 (3)	1093.162	0	3	5	0	C	
					(A)	1979.8	1141.848 (3)	1141.848	1	3	5	0	C, CoreF(1062.9), bisectGN(1273.8), BA-2	
					(A, C)	1254.7	1086.098 (3)	1086.099	1	5	4	2	H, CoreF(1254.5), (diSia(583.0))	
					(A)	1254.5	1628.644 (2)	1628.644	1	5	4	2	CoreF(1254.7)	
					(A, B)	1254.7	1115.437 (3)	1115.437	1	5	3	3	H, CoreF(1254.7), diSia(583.0)	
					(A)	1254.5	1672.651 (2)	1672.652	1	5	3	3	H, CoreF(1254.5), diSia(583.3)	
neurotrophin	AMDN <sup>127</sup> VTVR (904.444)	2	6, A2	h-1	2408 (A)	1254.5	1018.407 (3)	1018.405	1	5	3	2	H, CoreF(1254.5) or 512(512.2), diSia(582.6)	
					(A, C)	1254.7	1086.098 (3)	1086.099	1	5	4	2	C, CoreF(1254.5)	
					(A, B)	1254.7	1115.437 (3)	1115.437	1	5	3	3	H, CoreF(1254.7), diSia(583.0)	
					(A)	1254.5	1672.651 (2)	1672.652	1	5	3	3	H, CoreF(1254.5), diSia(583.3)	
					(A)	1254.6	1169.454 (3)	1169.455	1	6	3	3	H, CoreF(1254.6), diSia(583.0)	
					h-2	2473 (A, B, C)	1254.5	1183.131 (3)	1183.130	1	5	4	3	H, CoreF(1254.5) or 512(512.2), diSia(582.6)
					h-3	2719 (C)	1254.5	1280.163 (3)	1280.162	1	5	4	4	C, CoreF(1254.5), diSia(582.9) [Figure 6, A1]
					(C)	1108.6	1377.198 (3)	1377.194	1	5	4	5	Man-5	
					(B)	961.5	987.930 (2)	987.930	0	5	2	0	Man-6	
					(A, B, C)	3523 (A, B, C)	961.5	1068.956 (2)	1068.957	0	6	2	0	Man-7 [Figure 5, A1]
neurotrophin	VAWLN <sup>16</sup> R (757.424)	11	5, A2	a-1 (2)	3364 (A, B, C)	961.5	1149.986(2)	1149.983	0	7	2	0	Man-8	
				a-2 (2)	3221 (A, B, C)	961.5	1231.010 (2)	1231.010	0	8	2	0	Man-9	
				a-3 (2)	3413 (A, B, C)	961.5	1312.039 (2)	1312.036	0	9	2	0	glycosylated <sup>d</sup>	
				a-4 (2)	-	-	-	-	-	-	-	-	glycosylated <sup>d</sup>	
				(A)	6885 (A)	1159.4	1086.954 (2)	1086.951	0	5	2	0	glycosylated <sup>d</sup>	
				(A)	1159.4	1180.493 (2)	1180.494	1	4	3	0	Man-5		
				(A, B)	6824 (A, B)	1159.4	1201.011 (2)	1201.007	1	3	4	0	CoreF(1305.5)	
				(A)	1159.5	1261.520 (2)	1261.520	1	5	3	0	CoreF(1305.4)		
				(A, B)	6819 (A, B)	1159.4	1302.551 (2)	1302.546	1	3	5	0	H, CoreF(1305.3)	
				(A)	1159.5	1334.551 (2)	1334.549	2	5	3	0	C, CoreF(1305.3), bisectGN(864.6), BA-2		
neurotrophin	LTFN <sup>123</sup> VSE (955.465)	20	7, A2	k-4 (2)	6885 (A)	1159.4	1086.954 (2)	1086.951	0	5	2	0	H, CoreF(1305.3)	
				(A)	1159.4	1180.493 (2)	1180.494	1	4	3	0	H, CoreF(1305.3), 512(512.3)		
				(A, B)	6824 (A, B)	1159.4	1201.011 (2)	1201.007	1	3	4	0	CoreF(1305.2), 512(512.4)	
				(A)	1159.5	1261.520 (2)	1261.520	1	5	3	0	H, bisectGN(864.4), CoreF(1305.4) or 512(511.9)		
				(A, B)	6819 (A, B)	1159.4	1302.551 (2)	1302.546	1	3	5	0	H, CoreF(1305.4) or 512(511.9)	
				(A)	1159.5	1334.551 (2)	1334.549	2	5	3	0	H, CoreF(1305.3)		
				(A, B)	1159.4	1355.062 (2)	1355.062	2	4	4	0	H, CoreF(1305.2), 512(512.4)		
				(A, B)	1159.5	1363.059 (2)	1363.060	1	5	4	0	H, bisectGN(864.4), CoreF(1305.4) or 512(511.9)		
				(A)	1160.4	1407.068 (2)	1407.068	1	5	3	1	H, CoreF(1306.4)		
				(A)	1159.8	1415.576 (2)	1415.575	2	6	3	0	H, CoreF(1306.4)		

Table 1: Continued

protein	peptides		glycopeptides					N-glycan					
	sequence <sup>a,b</sup>	elution position	Figure	peak no. <sup>c</sup>	scan in Figure 4A <sup>d</sup>	observed peptide-related ion <sup>e</sup>	observed <i>m/z</i> in SIM mode <sup>b</sup>	theoretical <i>m/z</i> <sup>b</sup>	deduced monosaccharide composition				
									dHex	Hex	HexNAc	NA	deduced structure <sup>f</sup> (diagnostic ion)
L	YGN <sup>146</sup> YTCVASNK (1275.555)	5	7, B2	— (B)		1159.4	957.728 (3)	957.728	2	5	4	0	H, CoreF(1305.7), L <sup>M</sup> (350.3, 512.1)
				k-8 (2)	6735 (A, B)	1159.3	1436.093 (2)	1436.089	2	5	4	0	H, CoreF(1305.4), 512(512.3)
				— (A)		1159.7	1444.089 (2)	1444.086	1	6	4	0	H, CoreF(1305.4)
				— (B)		1159.5	971.404 (3)	971.404	2	4	5	0	C, CoreF(1305.4), 512(512.3)
				k-9 (2)	6725 (A, B)	1159.5	1456.605 (2)	1456.602	2	4	5	0	C, (CoreF(1305.4), 512(512.1)) or L <sup>M</sup> (658.2), bisectGN(864.3)
				— (A)		1160.6	1480.098 (2)	1480.097	2	5	3	1	H, CoreF(1305.3), sL <sup>M</sup> (454.3, 512.2, 657.1, 803.2)
				k-1	6590	1159.3	1006.417 (3)	1006.414	3	5	4	0	C, CoreF(1305.2), L <sup>M</sup> (658.3)
				k-2	6658	1159.4	1011.747 (3)	1011.746	2	6	4	0	H, CoreF(1305.3), L <sup>M</sup> (350.3, 512.1), bisectGN(865.4) [Figure 7, A1]
				— (A)		1159.3	1517.117 (2)	1517.115	2	6	4	0	H, CoreF(1305.3), 512(512.1)
				— (A, B)		1160.4	1019.749 (3)	1019.749	1	4	5	1	C, CoreF(1305.4)
				— (A)		1159.5	1054.760 (3)	1054.760	2	5	4	1	H, CoreF(1305.5), 512(512.2)
				k-3	6533	1159.5	1074.108 (3)	1074.107	3	5	5	0	C, CoreF(1305.4), L <sup>M</sup> (658.1)
				— (A)		1159.4	1087.442 (3)	1087.443	1	4	6	1	C, CoreF(1305.4)
				— (A)		1159.5	1122.453 (3)	1122.453	2	5	5	1	C, CoreF(1305.5), 512(512.2)
				k-5	6782 (A, B)	1159.4	1190.151 (3)	1190.146	2	5	6	1	C, CoreF(1305.3), sL <sup>M</sup> (350.2, 512.2, 657.1, 803.2)
				I-1	2954 (A, B, C)	1480.6	1078.100 (3)	1078.100	2	4	5	0	C, CoreF(1626.6), bisectGN(1024.9), L <sup>M</sup> (350.3, 512.1) [Figure 7, B1]
				I-1 (2)	2960 (A)	1479.5	1616.649 (2)	1616.647	2	4	5	0	C, CoreF(1626.6), bisectGN(1024.4), 512(512.2)
				I-2	2918 (A)	1479.6	1113.114 (3)	1113.111	3	5	4	0	H, CoreF(1625.5), L <sup>M</sup> (658.1)
				— (A)		1480.6	1126.446 (3)	1126.446	1	4	5	1	C, CoreF(1626.6)
				I-3	3093	1478.0	1161.457 (3)	1161.457	2	5	4	1	H, CoreF(1626.7), sL <sup>M</sup> (350.4, 512.1, 657.2, 803.1)
I-4	2905 (A, B)	1479.6	1180.806 (3)	1180.804	3	5	5	0	C, CoreF(1625.6), bisectGN(1024.6), L <sup>M</sup> (350.0, 512.3)				
HDYGN <sup>146</sup> YTCVASNK (1527.641)	8	—	3254 (A, C)	1732.4	1059.426 (3)	1059.425	1	3	5	0	C, CoreF(1878.7), bisectGN(1150.6), BA-2		
			3176 (A, C)	1731.6	1162.128 (3)	1162.129	2	4	5	0	C, (CoreF(1878.7), L <sup>M</sup> (350.1, 512.2)) or L <sup>M</sup> (658.4), bisectGN(1223.8)		

Table 1: Continued

protein	peptides sequence <sup>a,b</sup>	elution position	Figure	glycopeptides				N-glycan						
				peak no. <sup>c</sup>	scan in Figure 4A <sup>d</sup>	observed peptide- related ion <sup>e</sup>	observed <i>m/z</i> in SIM mode <sup>b</sup>	theoretical <i>m/z</i> <sup>b</sup>	deduced monosaccharide composition				deduced structure/ (diagnostic ion)	
									dHex	Hex	HexNAc	NA		
M	LGHTN <sup>773</sup> ASIMLFGPGAVSE (1799.888)	23	7, C2	m-1	— (C)	1732.7	1197.144 (3)	1197.139	3	5	4	0	H, CoreF(1877.7), L <sup>xy</sup> (512.2, 658.2), bisectGN(1149.1)	
					3439	1731.7	1210.475 (3)	1210.475	1	4	5	1	C, CoreF(1877.8), bisectGN(1222.6)	
					3383	1732.8	1245.488 (3)	1245.485	2	5	4	1	H, CoreF(1879.7), aL <sup>xy</sup> (453.9, 512.2, 657.2, 803.3)	
					3080 (C)	1732.7	1264.834 (3)	1264.833	3	5	5	0	C, CoreF(1878.7), bisectGN(1223.4), 512(512.1)	
					3553	1731.9	1293.835 (3)	1293.831	1	5	4	2	H, CoreF(1877.6), bisectGN(1150.5)	
					3560	1731.9	1294.175 (3)	1294.171	3	5	4	1	C, CoreF(1877.7)	
					7299 (C)	1002.6(2)	1101.491 (3)	1101.488	0	3	5	0	C, bisectGN(1286.7) [Figure 7, C1]	
					— (C)	1003.1(2)	1141.835 (3)	1141.830	0	5	4	0	H, bisectGN(1286.5)	
					m-2	7227 (C)	1002.6(2)	1150.176 (3)	1150.174	1	3	5	0	C, CoreF(1075.6), bisectGN(1357.6), BA-2
					m-3	7210	1002.7(2)	1190.520 (3)	1190.516	1	5	4	0	H, CoreF(1075.4) or 512(512.0), bisectGN(1359.1)
Kilon	N GAWLN <sup>38</sup> R (715.377)	3	8, A2	m-4	7186	1002.8(2)	1244.537 (3)	1244.534	1	6	4	0	H, 512(512.2)	
				— (B)	919.5	966.907 (2)	966.907	0	5	2	0	Man-5		
				n-1 (2)	2664 (A, B, C)	919.5	1047.934 (2)	1047.933	0	6	2	0	Man-6 [Figure 8, A1]	
				n-2 (2)	2706 (A, B, C)	919.5	1128.960 (2)	1128.960	0	7	2	0	Man-7	
				n-3 (2)	2679 (A, B, C)	919.4	1209.988 (2)	1209.986	0	8	2	0	Man-8	
				5234	972.3	1040.101 (3)	1040.102	0	6	2	0	Man-6		
O	CYLEDGASGAWLN <sup>38</sup> R (1738.810) GTN <sup>118</sup> VTLTCLATGKPE (1560.782)	18	—	o-1	4760	1765.8	1070.475 (3)	1070.472	1	3	5	0	C, CoreF(1910.8), bisectGN(1167.3), BA-2 [Figure 8, B1]	
				o-2	4683	1764.7	1105.485 (3)	1105.483	2	4	4	0	CoreF(1910.9), bisectGN(1167.8), 512(512.2)	
				o-3	4710 (C)	1765.7	1173.176 (3)	1173.176	2	4	5	0	C, CoreF(1911.9), bisectGN(1167.3), 512(512.1)	
				o-4	4638	1765.8	1275.880 (3)	1275.879	3	5	5	0	C, CoreF(1910.9), 512(512.1)	
				o-5	4857 (C)	1765.0	1324.227 (3)	1324.225	2	5	5	1	C, CoreF(1910.8), 512(512.1)	
				— (C)	1764.9	1401.911 (3)	1401.910	1	5	4	3	C, CoreF(1911.0)		
P	LFNGQQGIIIQN <sup>23</sup> FSTR (1834.969) RLFNGQQGIIIQN <sup>23</sup> FSTR (1991.070) KRLFNGQQGIIIQN <sup>23</sup> FSTR (2119.165)	22	8, C2	p-1	7203 (C)	1020.3(2)	1018.138 (3)	1018.138	0	5	2	0	Man-5 [Figure 8, C1]	
				—	6895 (C)	1098.3(2)	1070.171 (3)	1070.172	0	5	2	0	Man-5	
				—	6165 (C)	1162.4(2)	1112.871 (3)	1112.870	0	5	2	0	Man-5	
Q	SILTVTN <sup>24</sup> VTQE (1203.635)	17	8, D2	q-8 (2)	5086 (A, C)	1407.5	1211.037 (2)	1211.036	0	5	2	0	Man-5	
				— (B)	1407.7	883.729 (3)	883.730	1	3	4	0	CoreF(1553.5), bisectGN(1061.5)		

Table 1: Continued

protein	peptides sequence <sup>a,b</sup>	elution position	Figure	glycopeptides				N-glycan					
				peak no. <sup>c</sup>	scan in Figure 4A <sup>d</sup>	observed peptide- related ion <sup>e</sup>	observed <i>m/z</i> in SIM mode <sup>b</sup>	theoretical <i>m/z</i> <sup>b</sup>	deduced monosaccharide composition				deduced structure/ (diagnostic ion)
									dHex	Hex	HexNAc	NA	
R HFGN <sup>237</sup> YTCVAANK (1380.624)		10	8, E2	q-10 (2)	5059 (A, C)	1407.4	1325.094 (2)	1325.092	1	3	4	0	CoreF(1553.5) or 512(512.2), bisectGN(988.6)
				– (B)		1407.6	951.423 (3)	951.423	1	3	5	0	C, CoreF(1553.6), bisectGN(988.6), BA-2
				– (A)		1407.6	1426.632 (2)	1426.631	1	3	5	0	C, CoreF(1553.5), bisectGN(988.2), BA-2
				q-11 (2)	4950 (A, C)	1407.5	1458.635 (2)	1458.634	2	5	3	0	H, CoreF(1553.4), 512(512.2)
				– (B)		1407.3	991.765 (3)	991.765	1	5	4	0	H, CoreF(1553.6)
				– (A)		1407.6	1487.143 (2)	1487.144	1	5	4	0	H, CoreF(1553.4)
				q-1	5126 (A)	1407.5	1021.106 (3)	1021.104	1	5	3	1	H, CoreF(1553.4) or 512(512.2)
				– (A)		1407.6	1531.153 (2)	1531.152	1	5	3	1	H, CoreF(1553.6) or 512(512.0)
				q-2	4885 (C)	1407.4	1026.777 (3)	1026.776	2	6	3	0	H, CoreF(1553.5), L <sup>NA</sup> (350.3, 512.2)
				q-2 (2)	4919 (C)	1407.6	1539.663 (2)	1539.660	2	6	3	0	H, CoreF(1554.2), 512(512.1)
				q-3	5010 (A, C)	1407.5	1040.453 (3)	1040.451	2	5	4	0	H, CoreF(1553.6), L <sup>NA</sup> (350.2, 512.1)
				– (A)		1407.5	1560.174 (2)	1560.173	2	5	4	0	H, CoreF(1553.4), 512(512.2)
				q-4	4944 (A, C)	1406.6	1054.128 (3)	1054.127	2	4	5	0	C, CoreF(1552.6), L <sup>NA</sup> (350.2, 512.1) [Figure 8, D1]
				– (A)		1407.6	1580.687 (2)	1580.687	2	4	5	0	C, CoreF(1553.6), 512(512.2)
				– (A)		1407.5	1075.121(3)	1075.122	1	6	3	1	H, CoreF(1554.6)
				– (A)		1407.6	1612.180 (2)	1612.179	1	6	3	1	H, CoreF(1554.5)
				q-5	4827	1407.5	1089.139 (3)	1089.137	3	5	4	0	H, CoreF(1553.6), 512(512.1)
				– (A)		1407.5	1094.469 (3)	1094.469	2	6	4	0	H, CoreF(1554.3), L <sup>NA</sup> (350.3, 512.2)
				– (A)		1407.3	1102.473 (3)	1102.473	1	4	5	1	C, CoreF(1552.7)
				q-6	5032	1407.5	1137.486 (3)	1137.483	2	5	4	1	C, CoreF(1553.3), 512(512.2)
				q-7	4869 (A)	1407.6	1156.832 (3)	1156.830	3	5	5	0	C, CoreF(1553.5)
				– (A)		1407.6	1170.166 (3)	1170.166	1	4	6	1	C, CoreF(1553.3) or (sL <sup>NA</sup> 512.4, 803.6)
				q-9	5054 (A)	1407.4	1272.870 (3)	1272.869	2	5	6	1	C, CoreF(1553.5) (sL <sup>NA</sup> 454.1, 512.2, 657.2, 803.2))
– (B)		793.2(2)	866.690 (3)	866.690	0	5	2	0	Man-5				
r-7 (2)	3214 (C)	1584.7	1299.536 (2)	1299.531	0	5	2	0	Man-5				
r-1	3339 (C)	1584.6	1010.422 (3)	1010.420	1	3	5	0	C, CoreF(1730.6), bisectGN(1077.0), BA-2				
r-2	3162 (A, C)	1584.7	1050.764 (3)	1050.762	1	5	4	0	H, CoreF(1730.5), bisectGN(1077.7) [Figure 8, E1]				
r-3	3139 (A, C)	1585.9	1085.774 (3)	1085.772	2	6	3	0	H, CoreF(1730.8), L <sup>NA</sup> (350.2, 512.2)				

Table 1: Continued

protein	peptides sequence <sup>a,b</sup>	elution position	Figure	glycopeptides			N-glycan						
				peak no. <sup>c</sup>	scan in Figure 4A <sup>d</sup>	observed peptide- related ion <sup>e</sup>	observed <i>m/z</i> in SIM mode <sup>b</sup>	theoretical <i>m/z</i> <sup>b</sup>	deduced monosaccharide composition				deduced structure/ (diagnostic ion)
									dHex	Hex	HexNAc	NA	
				r-4	3208 (C)	1585.7	1099.450 (3)	1099.448	2	5	4	0	H, CoreF(1731.7), L <sup>Ma</sup> (350.1, 512.1)
				r-5	3189	1584.7	1104.784 (3)	1104.780	1	6	4	0	H, CoreF(1730.6) or L <sup>Ma</sup> (350.4, 512.0)
				r-6	3144 (A)	1585.6	1113.127 (3)	1113.123	2	4	5	0	C, CoreF(1730.8), L <sup>Ma</sup> (350.1, 512.2)
				-(A)		1585.8	1134.118 (3)	1134.118	1	6	3	1	H, CoreF(1730.6) or 512(512.3)
				-(A)		1584.5	1153.466 (3)	1153.466	2	6	4	0	H, CoreF(1731.6), L <sup>Ma</sup> (350.1, 512.2)

<sup>a</sup> Theoretical peptide mass indicated in parentheses. <sup>b</sup> Monoisotopic values. <sup>c</sup> Peaks are numbered in decreasing order of their calculated mass. All glycopeptides are triply charged except for doubly charged ions indicated by (2) after the peak number. <sup>d</sup> Glycopeptides were characterized on the basis of alternative LC-MS<sup>n</sup> runs with conditions indicated in parentheses (A, a C30 column, scan range of *m/z* 1000–2000; B, a C30 column, scan range of *m/z* 700–2000; C, a C18 column, scan range of *m/z* 1000–2000). <sup>e</sup> Y<sup>1+\*</sup> or Y<sup>1010\*</sup>, [(peptide + HexNAc + nH)/n]<sup>1+</sup>; or Y<sup>10\*</sup>, [(peptide + HexNAc + dHex + nH)/n]<sup>1+</sup>. All peptide-related ions are singly charged except for doubly or triply charged ions indicated by (2) or (3). <sup>f</sup> Structures are deduced by MS<sup>n</sup>: C, complex-type oligosaccharide; H, hybrid-type oligosaccharide; Man-5-9, high mannose-type oligosaccharide containing 5–9 mannose residues; CoreF, trimannosylcore fucose; bisectGN, bisecting GlcNAc; diSia, disialic acid; L<sup>Ma</sup>, Lewis a/x structure; sL<sup>Ma</sup>, sialylated Lewis a/x structure; L<sup>Ms</sup>, Lewis b/y structure; 512, glycan motif consisting of dHex<sub>1</sub>Hex<sub>1</sub>HexNAc<sub>1</sub>. The structure in parentheses indicates the possible structures to be contained in the glycopeptide. <sup>g</sup> Glycosylation was confirmed by Asn-Asp conversion upon PNGase F digestion.

integrated mass spectrum (peaks f-1–9 and g-1–3 in panel F2 of Figure 5) and their MS/MS spectra suggested that complex-type oligosaccharides including L<sup>Ma</sup> or L<sup>Ms</sup>-modified and/or bisected oligosaccharides and BA-2 are attached to Asn272 (Table 1F).

(vii) Asn287. The MS/MS spectra of GPI-linked peptides were selected from all MS data on the basis of the GPI-characteristic oxonium ions, such as GlcN-Ino-PO<sub>4</sub><sup>+</sup> (*m/z* 422). The structures of the GPI moieties were characterized from their product ions appearing in the MS/MS spectra, and their peptide portions were identified by comparing their observed masses with the theoretical masses of predicted peptides. Figure 4B shows the TIC obtained by GCC-LC-MS<sup>n</sup> for the hydrophilic glycopeptides. On the basis of the presence of GPI-characteristic oxonium ions, the MS data of GPI-linked peptides were located at position 26. The 9.5% of spectra generated at elution position 26 were assigned to those of GPI-linked peptides of LAMP, OBCAM, and neurotrophin.

Figure 5G shows one of the MS/MS spectra acquired at position 26 (precursor ion, [M + 2H]<sup>2+</sup> at *m/z* 902.5; peak L2 in Figure 4C). On the basis of the GPI-characteristic oxonium ions, such as NH<sub>2</sub>Et-PO<sub>4</sub>-Man-GlcN<sup>+</sup> (*m/z* 447.2), NH<sub>2</sub>Et-PO<sub>4</sub>-(HexNAc)-Man-GlcN<sup>+</sup> (*m/z* 650.3), NH<sub>2</sub>Et-PO<sub>4</sub>-(HexNAc)-Man-GlcN-Ino-PO<sub>4</sub><sup>+</sup> (*m/z* 910.2), NH<sub>2</sub>Et-PO<sub>4</sub>-(HexNAc)-(Hex)-Man-GlcN-Ino-PO<sub>4</sub><sup>+</sup> (*m/z* 1072.2), and GlcN-Ino-PO<sub>4</sub><sup>+</sup> (*m/z* 422.2), this peptide was identified as the GPI-linked peptide. The product ion at *m/z* 328.3 was assigned to GIN<sup>2+</sup>-NH-Et<sup>+</sup> on the basis of the fragments that arose by successive cleavages of HexNAc (*m/z* 1600.4), Ino-PO<sub>4</sub> (*m/z* 1340.5), GlcN (*m/z* 1178.3), Man-PO<sub>4</sub>-ENH<sub>2</sub> and Hex (*m/z* 732.2), Hex (*m/z* 570.2), and PO<sub>4</sub>-Hex (*m/z* 328.3). In addition, the product ions at *m/z* 732.3 and 1072.2 suggested the existence of HexNAc-(NH<sub>2</sub>Et-PO<sub>4</sub>)-(Hex)-Man3 in the core structure of GPI (inset of Figure 5G). The presence of a positional isomer was inferred from the acquisition of two different MS/MS spectra of GPI-linked peptides (precursor ion [M + 2H]<sup>2+</sup>, *m/z* 903) at different elution times (Table 2). The alternative runs also suggested the presence of a Hex-Man1 and HexNAc-(Hex)-(NH<sub>2</sub>Et-PO<sub>4</sub>)-Man3 (peak L1, data not shown, Table 2), and a nonsubstituted Man1 and HexNAc-(NH<sub>2</sub>Et-PO<sub>4</sub>)-Man3 (data not shown, Table 2) in the GPI core structure.

**Glycosylation Analysis of OBCAM.** OBCAM has six potential N-glycosylation sites at Asn17, -43, -113, -258, -266, and -279, and the predicted linkage site of GPI is Asn295. From the peptide-related ions, peptides eluted at positions 2, 25, and 7 were estimated to be glycopeptides containing Asn17, -258, and -266, respectively (panels A1–C1 of Figure 6). Panels A2–C2 of Figure 6 show the integrated mass spectrum of glycopeptides obtained from positions 2, 25, and 7, respectively. The glycopeptide containing Asn43 is identical to VAWLN<sup>28R</sup> in LAMP. From the glycosylation at Asn38 in LAMP, Man-5-9 were inferred to be attached to Asn43 (panel A2 of Figure 5 and Table 1A). Although the MS/MS spectrum of the glycopeptide containing Asn113 (VHLVQVPPQIMN<sup>113</sup>ISSD) was not acquired, glycosylation at Asn113 was corroborated by detection of VHLVQVPPQIMD<sup>113</sup>ISSD after PNGase F treatment (data not shown). The feature of glycosylation at Asn279 was elucidated on the basis of the MS/MS spectra of glycosylated LGNTN<sup>279</sup>ASITLLYGPQAVD which was

Table 2. Summary of GPI Structure in LAMP, OBCAM, and Neurotrimin

protein	peptide (theoretical MW <sup>a</sup> )	peak no. in Figure 4C	scan in Figure 4B	GPI-linked peptide		GPI moiety									
				observed peptide-related ion <sup>b</sup> (charge state)	observed <i>m/z</i> <sup>b</sup> (charge state)	calculated mass	deduced glycan composition						theoretical MW <sup>b</sup>		
							calculated mass	core	Hex	HexNAc	P-EtNH <sub>2</sub>				
LAMP	GIN <sup>187</sup> (302.3)	L1	3863	328.3 (1)	983.6 (2)	1965.1	1680.9	1	1	1	1	1	1681.3		
			L2	3828 <sup>c</sup> (Figure 5G)	328.3 (1)	902.5 (2)	1803.0	1518.8	1	0	1	1	1	1519.2	
				4040 <sup>d</sup>	328.3 (1)	903.1 (2)	1804.2	1520.0	1	0	1	1	1	1519.2	
				a	328.2 (1)	821.6 (2)	1641.1	1356.9	1	0	0	1	1	1	1357.0
					3701 (Figure 6D)	314.3 (1)	976.5 (2)	1951.0	1680.7	1	1	1	1	1	1681.3
OBCAM	GVN <sup>295</sup> (288.3)	O1	3633 <sup>d</sup>	314.3 (1)	895.4 (2)	1788.7	1518.4	1	0	1	1	1	1519.2		
			O2	3853 <sup>d</sup>	314.3 (1)	895.5 (2)	1788.9	1518.6	1	0	1	1	1	1519.2	
				3805	314.3 (1)	814.6 (2)	1627.1	1356.8	1	0	0	1	1	1357.0	
				O3	3750	371.2 (1)	1004.8 (2)	2007.7	1680.3	1	1	1	1	1	1681.3
					3741 <sup>e</sup>	371.4 (1)	924.0 (2)	1846.1	1518.7	1	0	1	1	1	1519.2
neurotrimin	VNN <sup>289</sup> (345.4)	N1	3896 <sup>e</sup>	371.2 (1)	924.1 (2)	1846.1	1518.8	1	0	1	1	1	1519.2		
			N2	3873 (Figure 7D)	371.3 (1)	842.8 (2)	1683.5	1356.1	1	0	0	1	1	1357.0	

<sup>a</sup> The structure of GPI was deduced by another LC-MS<sup>n</sup> run. <sup>b</sup> Average value. <sup>c</sup> Isomers. <sup>d</sup> Isomers. <sup>e</sup> Isomers.

acquired in an alternative run with the C30 column (scan range of *m/z* 1000–2000) (Table 1J).

(i) *Asn 17*. As shown in panel A1 of Figure 6, the glycopeptide that eluted at position 2 was assigned to AMDN<sup>17</sup>VTVR (and/or AMDN<sup>12</sup>VTVR in neurotrimin) glycosylated with dHex<sub>3</sub>Hex<sub>3</sub>HexNAc<sub>2</sub>NeuAc<sub>2</sub> based on the Y<sub>16</sub> ion and the monoisotopic mass of the molecular ion. The attachment of three NeuAc residues in one branch of a biantennary complex type was suggested by the existence of characteristic B ions (*m/z* 495.2, 744.9, and 1239.2) (panel A1 of Figure 6). The molecular ions appearing in the integrated mass spectrum and their MS/MS spectra suggested that most of the glycans at *Asn 17* were disialic acid-conjugated oligosaccharides [peaks h-1–3 in panel A2 of Figure 6 and Table 1(G)].

(ii) *Asn 258*. Panel B1 of Figure 6 shows the representative MS/MS spectrum of glycosylated ISTLTFN<sup>258</sup>VSE that eluted at position 25. The monosaccharide composition (dHex<sub>3</sub>Hex<sub>3</sub>HexNAc<sub>2</sub>NeuAc<sub>1</sub>) implied two possible structures: a sLe<sup>x</sup>-modified core-fucosylated complex type and a Le<sup>x</sup> or antigen H-modified core-fucosylated and sialylated complex type (inset of panel B1 of Figure 6). The molecular ions (peaks i-1–2) in the integrated mass spectrum (panel B2 of Figure 6) and the detection of nonglycosylated ISTLTFN<sup>258</sup>VSE revealed that *Asn 258* is partly glycosylated with the sLe<sup>x</sup> or Le<sup>x</sup>-modified core-fucosylated complex type, and BA-2 (Table 1H).

(iii) *Asn 266*. Panel C1 of Figure 6 shows the product ion spectra of the glycopeptide at position 7, the peptide portion of which was assigned to YGN<sup>266</sup>YTCVATNK on the basis of the Y<sub>16</sub> ion in the MS/MS spectrum. The glycan was characterized as the bisected and core-fucosylated complex-type oligosaccharide containing Le<sup>x</sup> structure from the monosaccharide composition (dHex<sub>3</sub>Hex<sub>3</sub>HexNAc<sub>3</sub>) and the Le<sup>x</sup>, bisecting-, and core-fucose-related ions. The MS/MS spectra acquired with other glycoforms (peaks j-1–4 in panel C2 of Figure 6) together with the MS/MS spectra of the glycopeptides DYGN<sup>266</sup>YTCVATNK (position 13) and KDYGN<sup>266</sup>YTCVATNK (position 6) suggested that the Le<sup>x</sup>-modified and/or bisected complex type and Man-5 were predominantly attached to *Asn 266* (Table 1I).

(iv) *Asn 295*. On the basis of the GPI-characteristic oxonium ions and the peptide-related ion (*m/z* 314.3), the MS/MS spectrum of GPI-linked GVN<sup>295</sup> was picked out from position 26 (Figure 6D; precursor ion, *m/z* 976.5; peak O1 in Figure 4C). The fragments arising from the GPI moiety suggested the linkage of Hex to Man1, and HexNAc, Hex, and NH<sub>2</sub>Et-PO<sub>4</sub> to Man3 in the core structure (Figure 6D, inset). Furthermore, the MS/MS spectrum of other GPI-linked GVN<sup>295</sup> (precursor ion, *m/z* 895; peak O2), which was picked out from position 26 based on the peptide-related ion, suggested that this GPI moiety contained HexNAc-(Hex)-(NH<sub>2</sub>Et-PO<sub>4</sub>)-Man3. Another MS/MS spectrum (precursor ion, *m/z* 814; peak O3) suggested the linkage of GPI moieties containing HexNAc-(NH<sub>2</sub>Et-PO<sub>4</sub>)-Man3 (Table 2). The existence of two isomers was suggested in peak O2 by the acquisition of two MS/MS spectra of GPI-GVN<sup>295</sup> (*m/z* 895) at different elution times.

*Glycosylation Analysis of Neurotrimin*. Neurotrimin contains seven potential N-glycosylation sites at *Asn 12*, -38, -120, -184, -252, -260, and -273, and the predicted linkage site of GPI is *Asn 289*. As the amino acid sequence in the

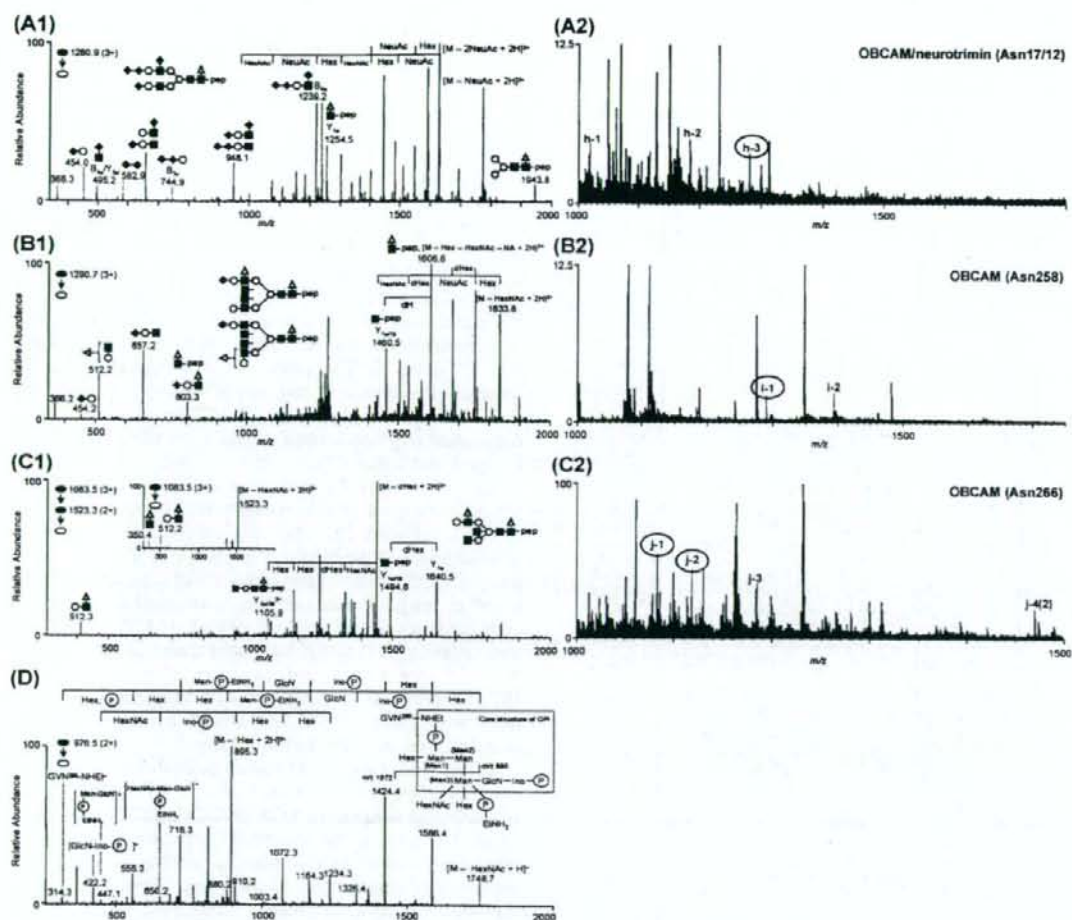


FIGURE 6: MS spectra of OBCAM glycopeptides. (A1) MS/MS spectra of glycopeptide AMDN<sup>17</sup>VTVR; elution position, 2; precursor ion, [M + 3H]<sup>3+</sup> (*m/z* 1280.9). (A2) Integrated mass spectrum obtained from position 2. (B1) MS/MS spectrum of glycopeptide ISLTFFN<sup>25</sup>VSE; elution position, 25; precursor ion, [M + 3H]<sup>3+</sup> (*m/z* 1290.7). (B2) Integrated mass spectrum at position 25. (C1) MS/MS and MS/MS/MS spectra of glycopeptide YGN<sup>266</sup>YTCVATNK; elution position, 7; precursor ion, [M + 3H]<sup>3+</sup> (*m/z* 1083.5). (C2) Integrated mass spectrum at position 7. (D) MS/MS spectrum of GPI-linked GVN<sup>295</sup>; elution position, 26; precursor ion, [M + 2H]<sup>2+</sup> (*m/z* 976.5). Symbols are as in Figure 9.

glycopeptide containing Asn12 (GTDN<sup>12</sup>ITVR) in neurotrimin is identical to GTDN<sup>17</sup>ITVR in OBCAM, the glycans at Asn12 are estimated to be hybrid and complex types containing disialic acid (panel A2 of Figure 6 and Table 1G). Likewise, the sequence of VAWLN<sup>38</sup>R in neurotrimin is identical to that of VAWLN<sup>38</sup>R in LAMP, and therefore, the linkage of Man-5-9 at Asn38 was inferred from the glycosylation at Asn38 in LAMP (panel A2 of Figure 5 and Table 1A). Although the MS/MS spectra of glycopeptides containing Asn120 were not acquired, glycosylation at Asn120 was confirmed by the identification of GND<sup>120</sup>ISLTLCIATGR, GND<sup>120</sup>ISLTLCIATGRPE, and GND<sup>120</sup>ISLTLCIATGRPEPTWTWR after PNGase F digestion (data not shown). The substitution of Asn184 with a Lys or an Arg residue in neurotrimin was suggested as in case of SD rat by the identification of VTVNYPPISE, which is a fragment of VN<sup>184</sup>VTNYPPISE (data not shown) (33).

The MS/MS spectra of glycopeptides containing Asn252, -260, -273, and -289 were located at positions 20, 5, 23, and 26 based on the peptide-related ions, respectively (panels A1–C1 and D of Figure 7). The integrated mass spectrum of the glycopeptides containing Asn252, -260, and -273 are shown in panels A2–C2 of Figure 7, respectively.

(i) *Asn252*. Panel A1 of Figure 7 shows the representative MS/MS spectra of glycopeptide LTFFN<sup>252</sup>VSE linked by dHex<sub>2</sub>Hex<sub>6</sub>HexNAc<sub>4</sub>, acquired at position 20. A Le<sup>bx</sup>-modified core-fucosylated and bisected hybrid-type oligosaccharide was deduced from the Le<sup>bx</sup>-related ions, and Y<sub>1β3α3β</sub><sup>2+</sup> and Y<sub>1α</sub>. The majority of the glycans at Asn252 are estimated to be Le<sup>bx</sup> or Le<sup>by</sup>-modified complex- and hybrid-type oligosaccharides from the molecular ions (peaks k-1–9) in the integrated mass spectrum and their MS/MS spectra (panel A2 of Figure 7 and Table 1K).



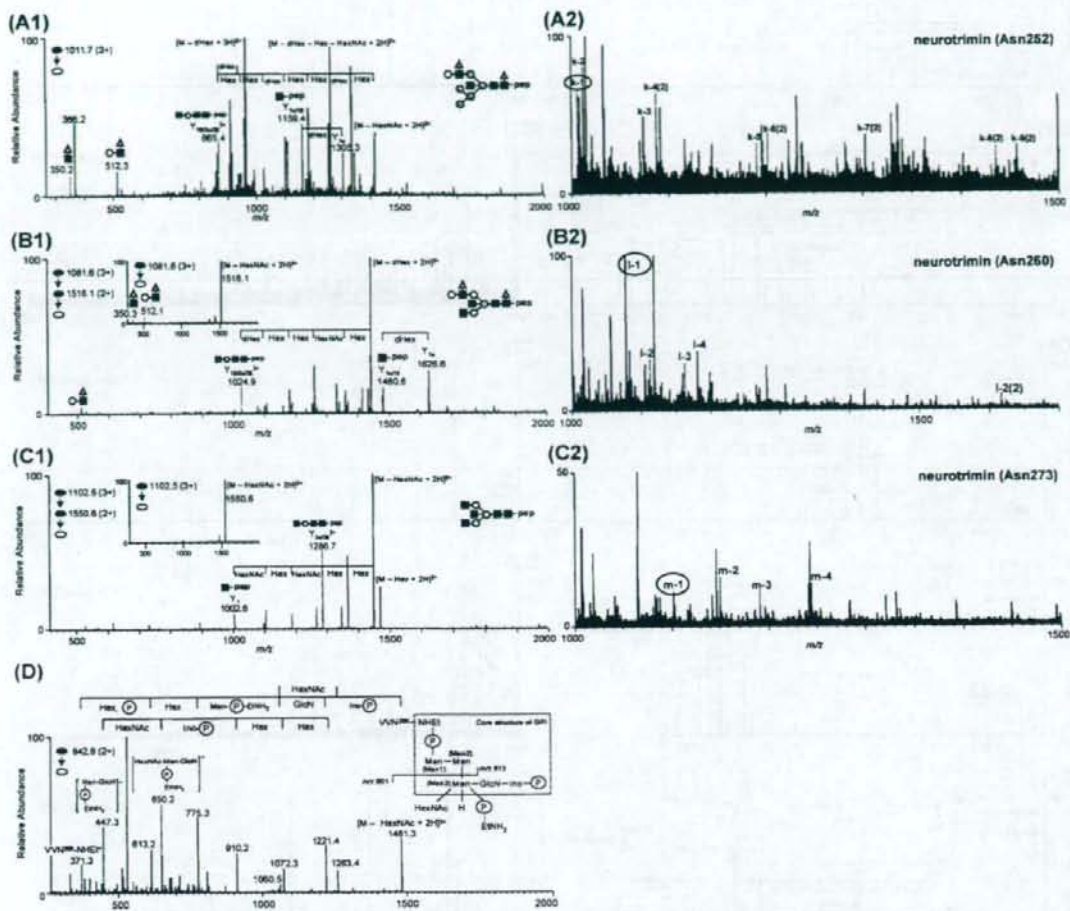


FIGURE 7: MS spectra of neurotrophin glycopeptides. (A1) MS/MS spectra of glycopeptide LTFN<sup>257</sup>VSE; elution position, 20; precursor ion,  $[M + 3H]^{3+}$  ( $m/z$  1011.7). (A2) Integrated mass spectrum obtained from position 20. (B1) MS/MS and MS/MS/MS spectra of glycopeptide YGN<sup>260</sup>YTCVASNK; elution position, 5; precursor ion,  $[M + 3H]^{3+}$  ( $m/z$  1081.6). (B2) Integrated mass spectrum at position 5. (C1) MS/MS and MS/MS/MS spectra of glycopeptide LGHTN<sup>273</sup>ASIMLFGPGAVSE; elution position, 23; precursor ion,  $[M + 3H]^{3+}$  ( $m/z$  1102.5). (C2) Integrated mass spectrum at position 23. (D) MS/MS spectrum of GPI-linked VNN<sup>289</sup>; elution position, 26; precursor ion,  $[M + 2H]^{2+}$  ( $m/z$  842.8). Symbols are as in Figure 9.

(ii) *Asn260*. Panel B1 of Figure 7 shows the representative product ion spectra of the glycopeptide eluted at position 5, the peptide portion of which was identified as YGN<sup>260</sup>YTCVASNK on the basis of the  $Y_{10/11}$  ion in the MS/MS/MS spectrum. The monosaccharide composition (dHex<sub>2</sub>Hex<sub>4</sub>HexNAc<sub>5</sub>), the Le<sup>ax</sup>-related ions in the MS/MS spectrum, and the presence of  $Y_{11/10}$  and  $Y_{10}$  in the MS/MS/MS spectrum revealed the linkage of a Le<sup>ax</sup>-modified fucosylated and bisected complex-type oligosaccharide to this peptide (inset of panel B1 of Figure 7). The molecular ions in the integrated mass spectrum (peaks 1-1-4 in panel B2 of Figure 7) together with the MS/MS spectra of glycosylated HDYGN<sup>260</sup>YTCVASNK (position 8) suggested that Asn260 was predominantly glycosylated with the Le<sup>ax</sup> or Le<sup>bx</sup>-modified bisected complex- and hybrid-type oligosaccharides and BA-2 (Table 1L).

(iii) *Asn273*. On the basis of the  $Y_1$  ion and the monoisotopic mass, the glycopeptide eluted at position 23 was assigned to LGHTN<sup>273</sup>ASIMLFGPGAVSE glycosylated with Hex<sub>3</sub>HexNAc<sub>5</sub> (panel C1 of Figure 7). Its glycan moiety was characterized as a bisected agalacto-complex-type oligosaccharide based on  $Y_{3a/b}^{2+}$ . Other glycans at Asn273 were assigned to bisected complex- and hybrid-type oligosaccharides (peaks m-1-4 in panel C2 of Figure 7 and Table 1M).

(iv) *Asn289*. Figure 7D shows one of the MS/MS spectra of GPI-linked VNN<sup>289</sup>, which was picked out from position 26 on the basis of the peptide-related ion (peptide-NH-Er<sup>+</sup>,  $m/z$  371.3). Three different MS/MS spectra of GPI-linked VNN<sup>289</sup> were picked out from position 26 (Figure 4B). From the molecular ions [peaks N1 ( $m/z$  1004), N2 ( $m/z$  924), and N3 ( $m/z$  842)] and their fragments, it was suggested that they contain Hex-Man1 and HexNAc-(Hex-)(NH<sub>2</sub>Et-PO<sub>4</sub>-)Man<sub>3</sub>,

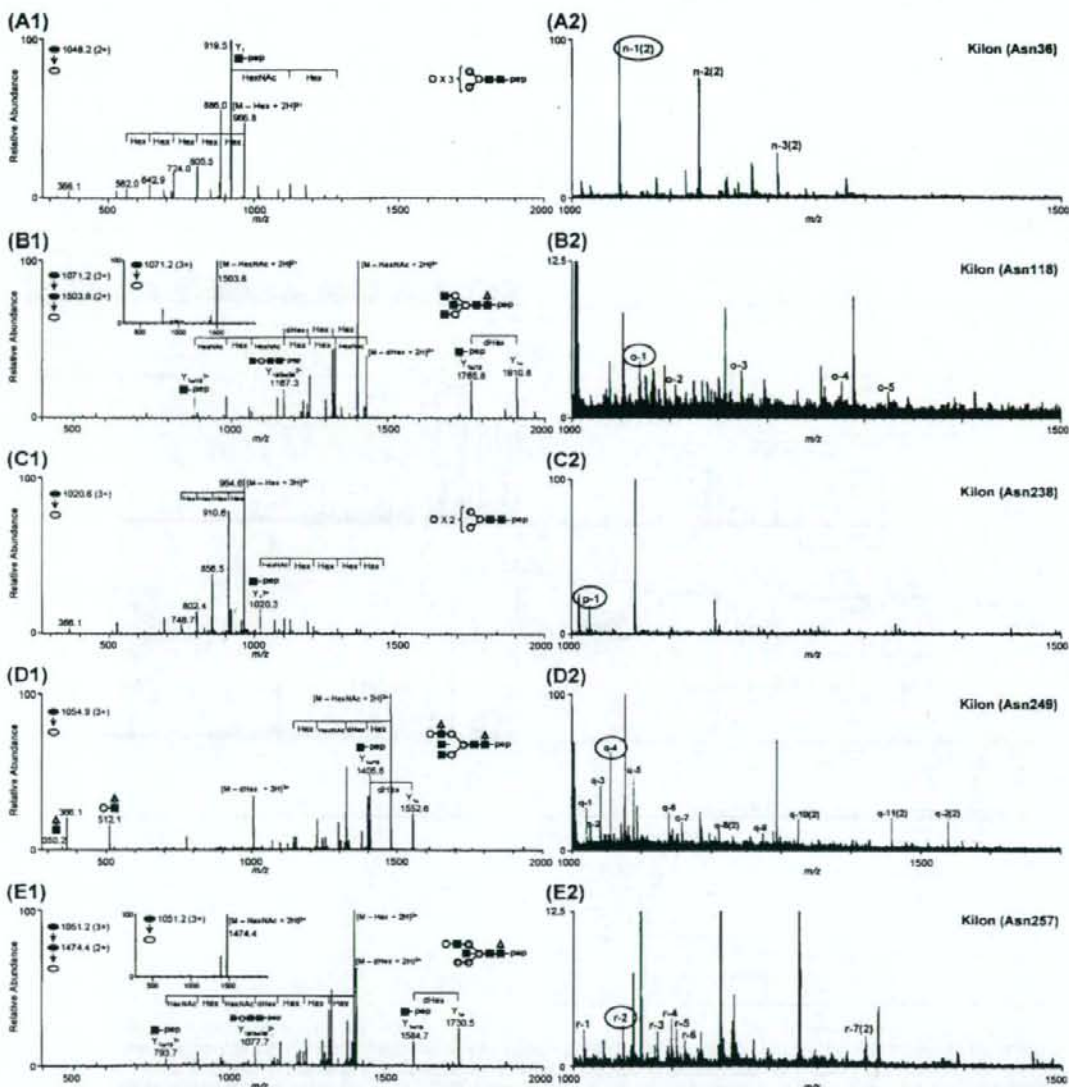


FIGURE 8: MS spectra of Kilon glycopeptides. (A1) MS/MS spectra of glycopeptide GAWLN<sup>36</sup>R; elution position, 3; precursor ion,  $[M + 2H]^{2+}$  ( $m/z$  1048.2). (A2) Integrated mass spectrum obtained from position 3. (B1) MS/MS and MS/MS/MS spectra of glycopeptide GTN<sup>118</sup>VTLTCLATGKPE; elution position, 16; precursor ion,  $[M + 3H]^{3+}$  ( $m/z$  1071.2). (B2) Integrated mass spectrum at position 16. (C1) MS/MS spectrum of glycopeptide LFNQQGIIQIN<sup>238</sup>FSTR; elution position, 22; precursor ion,  $[M + 3H]^{3+}$  ( $m/z$  1020.6). (C2) Integrated mass spectrum at position 22. (D1) MS/MS spectrum of glycopeptide SILTVTN<sup>249</sup>VTQE; elution position, 17; precursor ion,  $[M + 3H]^{3+}$  ( $m/z$  1054.9). (D2) Integrated mass spectrum at position 17. (E1) MS/MS and MS/MS/MS spectra of glycopeptide HFGN<sup>257</sup>YTCVAANK; elution position, 10; precursor ion,  $[M + 3H]^{3+}$  ( $m/z$  1051.2). (E2) Integrated mass spectrum at position 10. Symbols are as in Figure 9.

HexNAc-(Hex)-(NH<sub>2</sub>Et-PO<sub>4</sub>)Man<sub>3</sub>, and HexNAc-(NH<sub>2</sub>Et-PO<sub>4</sub>)Man<sub>3</sub>, respectively. The existence of two isomers was suggested in peak N2 by the presence of two different MS/MS spectra at different elution times (Table 2).

**Glycosylation Analysis of Kilon.** Kilon has six potential N-glycosylation sites at Asn36, -118, -238, -249, -257, and -270. The predicted linkage site of GPI is Gly287. The typical MS/MS spectra and the integrated mass spectra of the glycopeptides containing Asn36, -118, -238, -249, and -257

are shown in panels A1–E1 and A2–E2 of Figure 8, respectively. The MS/MS spectra of the glycopeptide containing both Asn270 and Gly287 could not be picked out from the MS data.

(i) *Asn36.* Panel A1 of Figure 8 shows one of the MS/MS spectra acquired at position 3. This glycopeptide was identified as GAWLN<sup>36</sup>R with Man-6 based on Y<sub>1</sub> ion and the monosaccharide composition. Other glycans at Asn36 were estimated as Man-5, -7, and -8 from the existence of

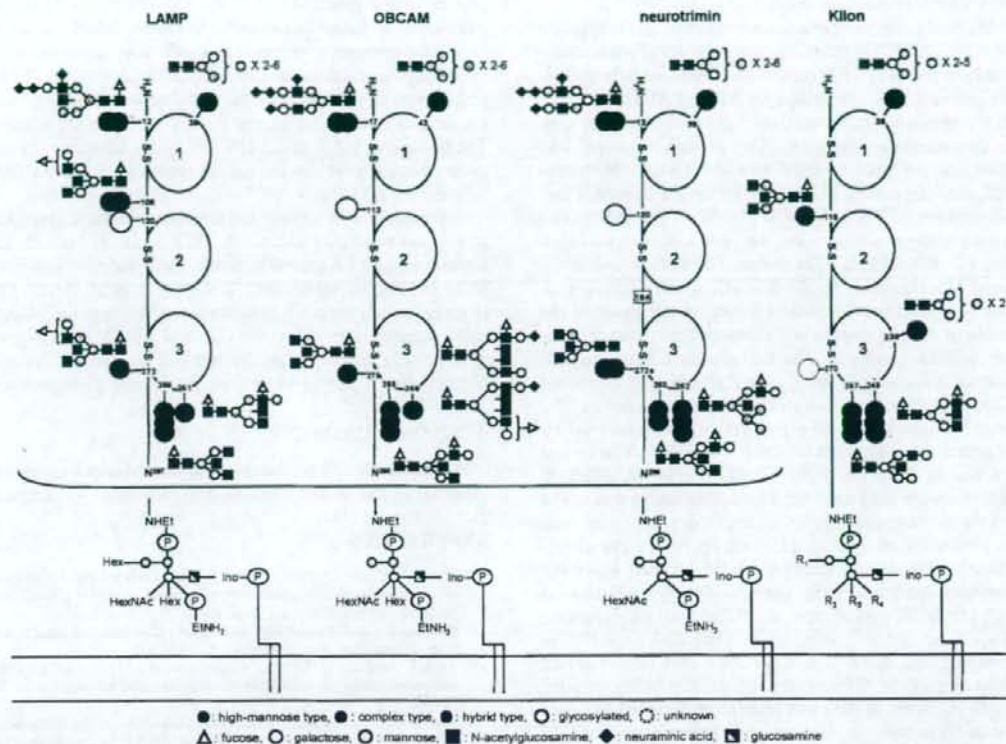


FIGURE 9: Summary of glycosylation of IgLON family proteins.

molecular ions with 81  $m/z$  units intervals in the integrated mass spectrum (peaks n-1–3 in panel A2 of Figure 8) (Table 1N).

(ii) *Asn118*. As shown in panel B1 of Figure 8, the MS/MS spectrum acquired at position 16 contained  $Y_{1\alpha/1\beta}$ , which suggested that the peptide portion is  $GTN^{118}VTLTCLATGKPE$ . The linkage of BA-2 was deduced from the monosaccharide composition ( $dHex_1Hex_3HexNAc_5$ ), and  $Y_{1\beta/3\alpha/3\beta}^{2+}$  and  $Y_{1\alpha}$  (inset of panel B1 of Figure 8). Additionally, the linkage of  $Le^{Mx}$  or antigen H-modified and/or bisected complex type was suggested by the integrated mass spectrum (peaks o-1–5 in panel B2 of Figure 8 and Table 1O).

(iii) *Asn238*. The MS/MS spectra of glycopeptides that contain Asn238 were picked out from positions 22 [LFNGQQGIIIQN<sup>238</sup>FSTR (panel C1 of Figure 8)], 21 [RLFNGQQGIIIQN<sup>238</sup>FSTR], and 19 [KRLFNGQQGIIIQN<sup>238</sup>FSTR]. These MS/MS spectra and molecular ions appearing in the integrated mass spectrum revealed that the only carbohydrate structure at Asn238 was Man-5 (peak p-1 in panel C2 of Figure 8 and Table 1P). Together with the results of the database search analysis, in which nonglycosylated peptide LFNGQQGIIIQN<sup>238</sup>FSTR was identified, it was suggested that Man-5 was partly attached to Asn238 (Table 1P).

(iv) *Asn249*. Panel D1 of Figure 8 shows the representative MS/MS spectrum of glycopeptide SILTVTN<sup>249</sup>VTQE at position 17. The carbohydrate structure was characterized as a  $Le^{Mx}$ -modified and core-fucosylated complex type by

the existence of the  $Le^{Mx}$ -related ions and  $Y_{1\alpha}$ . The integrated mass spectrum and alternative LC-MS<sup>n</sup> with the C30 column (scan ranges of  $m/z$  700–2000 and 1000–2000) suggested that Asn249 is glycosylated with  $Le^{Mx}$  or antigen H-modified core-fucosylated hybrid- and complex-type oligosaccharides, BA-2, and Man-5 (peaks q-1–11 in panel D2 of Figure 8 and Table 1Q).

(v) *Asn257*. As shown in panel E1 of Figure 8, one of the glycopeptides eluted at position 10 was identified as HFGN<sup>257</sup>YTCVAANK linked by  $dHex_1Hex_3HexNAc_4$  based on  $Y_{1\alpha/1\beta}$  ion in the MS/MS/MS spectra and monoisotopic mass. The carbohydrate structure was characterized as a bisected- and core-fucosylated hybrid-type oligosaccharide based on the presence of  $Y_{1\beta/3\alpha/3\beta}^{2+}$  and  $Y_{1\alpha}$  (inset of panel E2 of Figure 8). Other major glycans were estimated as Man-5,  $Le^{Mx}$ -modified complex- and hybrid-type oligosaccharides, and BA-2 (peaks r-1–7 in panel E2 of Figure 8 and Table 1R).

## DISCUSSION

The cell adhesion molecules in the central nervous system play an essential role in the differentiation of neuronal cells and formation of neural circuits. Although glycosylation on the cell adhesion molecules is known to regulate cell–cell interactions (2–4), their carbohydrate structures remain unknown due to the difficulty with respect to their isolation and the limited sample amounts. The glycans in the IgLON family proteins are considered to be implicated in the

formation of neural circuits, including migration of neuronal cells, axonal guidance, and fasciculation. However, the high degree of homology of their amino acid sequences makes it difficult to isolate them from each other and to analyze their carbohydrate structures in detail.

In this study, we performed a site-specific glycosylation analysis of LAMP, OBCAM, neurotrimin, and Kilon simultaneously using SDS-PAGE and LC-MS<sup>n</sup>. Enriched GPI-linked proteins were separated by SDS-PAGE, and four target proteins were extracted from a gel piece together with other contaminating proteins. The protein mixture was digested and analyzed by the C30 and C18-LC-MS<sup>n</sup> runs via MS, data-dependent MS in SIM by the FT ICR-MS, and data-dependent MS/MS and MS/MS/MS. A set of MS data consisting of the mass spectrum, the mass spectrum acquired by the FT ICR-MS in SIM mode, the data-dependently acquired MS/MS, and the MS/MS/MS spectra of a glycopeptide was selected from all MS data on the basis of the existence of the oligosaccharide characteristic oxonium ions in the MS/MS spectrum. The carbohydrate structure and peptide sequence were deduced from the carbohydrate-related ions and peptide-related ions in the product ion spectra. The structural assignment of the glycopeptide was confirmed by the accurate mass acquired on the FT ICR-MS. The b- and y-ions arising from the peptide backbone in the MS/MS/MS spectra were also used for the peptide assignment. The carbohydrate heterogeneity at each glycosylation site was characterized by integrating the mass spectra of the glycopeptides which yielded identical peptide-related ions. We successfully determined the site-specific glycosylation in LAMP, OBCAM, neurotrimin, and Kilon with the exception of Asn120 in LAMP, Asn113 in OBCAM, Asn120 in neurotrimin, and Asn270 in Kilon. We also demonstrated the structure of the GPI moiety using LC-MS<sup>n</sup> equipped with a GCC. A set of data was picked out from all MS data by using GPI-characteristic ions, and the structure of GPI and the linkage site were deduced from the product ions in the MS/MS spectra. Three different structures are commonly found in LAMP, OBCAM, and neurotrimin.

Figure 9 illustrates the site-specific glycosylation in the four proteins. N-Glycosylation sites near the N-terminus in LAMP, OBCAM, and neurotrimin were commonly occupied with biantennary complex-type and hybrid-type oligosaccharides containing disialic acids. Oligosialic acids and disialic acids, which are found in several glycoproteins, including NCAM, are considered to regulate the cell-cell interaction by changing their degree of polymerization (6). Disialic acids at the near N-terminus in LAMP, OBCAM, and neurotrimin might regulate the cell-cell interaction in a manner similar to that of other glycosylated adhesion molecules.

The first domains in IgLON family proteins are commonly glycosylated with Man-5, -6, -7, -8, and -9. The linkage of high-mannose-type oligosaccharides is found in several Ig superfamily proteins, including L1, MAG, and P0 (3). Since Horstkorte et al. have reported that L1 binds to NCAM through oligomannosidic carbohydrates in L1 (34), the high-mannose-type oligosaccharide in IgLON family proteins could interact with certain biological molecules.

The third domains of all IgLON proteins were highly heterogeneous due to a linkage of diverse oligosaccharides, including BA-2, the Le<sup>ax</sup> or Le<sup>bx</sup> motif, and Man-5. BA-2,

a bisected agalacto-complex type, is known as a brain-specific glycan and is much more abundant in mammalian brains than in other tissues (35, 36). Recently, the Na<sup>+</sup>/K<sup>+</sup>-ATPase  $\beta$ 1 subunit was identified as a GlcNAc-binding protein in the mouse brain (37). The Na<sup>+</sup>/K<sup>+</sup>-ATPase  $\beta$ 1 subunit is a potassium-dependent lectin which binds to GlcNAc-terminating oligosaccharides and is involved in neural cell interactions in a trans-binding fashion. A 74 kDa protein was suggested to be the GlcNAc-terminating glycan carrier protein binding to the Na<sup>+</sup>/K<sup>+</sup>-ATPase  $\beta$ 1 subunit. The linkage of BA-2 to IgLON family proteins implies that these proteins might be the ligand proteins for the Na<sup>+</sup>/K<sup>+</sup>-ATPase  $\beta$ 1 subunit.

Glycosylation in a great number of membrane glycoproteins remains largely unknown. This is mainly because the limited amount of available sample and the low solubility of glycoproteins make their isolation quite difficult. Our strategy, which includes enrichment of the target glycoproteins, separation by SDS-PAGE, and LC-MS<sup>n</sup> of digests of a protein mixture, can be applied to the site-specific glycosylation analysis of various membrane glycoproteins.

#### ACKNOWLEDGMENT

We thank Dr. Masayuki Kubota and Morihiko Yoshida (Thermo Fisher Scientific K.K.) for their technical support.

#### REFERENCES

- Walsh, F. S., and Doherty, P. (1997) Neural cell adhesion molecules of the immunoglobulin superfamily: Role in axon growth and guidance. *Annu. Rev. Cell Dev. Biol.* 13, 425-456.
- Kleene, R., and Schachner, M. (2004) Glycans and neural cell interactions. *Nat. Rev. Neurosci.* 5, 195-208.
- Krog, L., and Bock, E. (1992) Glycosylation of neural cell adhesion molecules of the immunoglobulin superfamily. *APMIS, Suppl.* 27, 53-70.
- Schachner, M., and Martini, R. (1995) Glycans and the modulation of neural-recognition molecule function. *Trends Neurosci.* 18, 183-191.
- Liedtke, S., Geyer, H., Wührer, M., Geyer, R., Frank, G., Gerardy-Schahn, R., Zahring, U., and Schachner, M. (2001) Characterization of N-glycans from mouse brain neural cell adhesion molecule. *Glycobiology* 11, 373-384.
- Rutishauser, U. (1996) Polysialic acid and the regulation of cell interactions. *Curr. Opin. Cell Biol.* 8, 679-684.
- Kunemund, V., Jungalwala, F. B., Fischer, G., Chou, D. K., Keilhauer, G., and Schachner, M. (1988) The L2/HNK-1 carbohydrate of neural cell adhesion molecules is involved in cell interactions. *J. Cell Biol.* 106, 213-223.
- Cho, T. M., Hasegawa, J., Ge, B. L., and Loh, H. H. (1986) Purification to apparent homogeneity of a  $\mu$ -type opioid receptor from rat brain. *Proc. Natl. Acad. Sci. U.S.A.* 83, 4138-4142.
- Funatsu, N., Miyata, S., Kumanogoh, H., Shigeta, M., Hamada, K., Endo, Y., Sokawa, Y., and Maekawa, S. (1999) Characterization of a novel rat brain glycosylphosphatidylinositol-anchored protein (Kilon), a member of the IgLON cell adhesion molecule family. *J. Biol. Chem.* 274, 8224-8230.
- Levitt, P. (1984) A monoclonal antibody to limbic system neurons. *Science* 223, 299-301.
- Pimenta, A. F., Zhukareva, V., Barbe, M. F., Reinoso, B. S., Grimley, C., Henzel, W., Fischer, I., and Levitt, P. (1995) The limbic system-associated membrane protein is an Ig superfamily member that mediates selective neuronal growth and axon targeting. *Neuron* 15, 287-297.
- Schofield, P. R., McFarland, K. C., Hayflick, J. S., Wilcox, J. N., Cho, T. M., Roy, S., Lee, N. M., Loh, H. H., and Seeburg, P. H. (1989) Molecular characterization of a new immunoglobulin superfamily protein with potential roles in opioid binding and cell contact. *EMBO J.* 8, 489-495.
- Struyk, A. F., Canoll, P. D., Wolfgang, M. J., Rosen, C. L., D'Eustachio, P., and Salzer, J. L. (1995) Cloning of neurotrimin